AMMRC MS 83-1

THE MEASUREMENT OF RESIDUAL STRESS WITH X-RAY DIFFRACTION

CHARLES P. GAZZARA
MATERIALS CHARACTERIZATION DIVISION

May 1983

ARMY MATERIALS AND MECHANICS RESEARCH CENTER
Watertown, Massachusetts 02172

The findings in this report are not to be construed as an official Department of the Army position, unless so designated by other authorized documents.

Mention of any trade names or manufacturers in this report shall not be construed as advertising nor as an official indorsement or approval of such products or companies by the United States Government.

DISPOSITION INSTRUCTIONS

Destroy this report when it is no longer needed.
Do not return it to the originator.

UNCLASSIFIED

SECURITY CLASSIFICATION OF THIS PAGE *(When Data Entered)*

REPORT DOCUMENTATION PAGE

READ INSTRUCTIONS BEFORE COMPLETING FORM

1. REPORT NUMBER: AMMRC MS 83-1	2. GOVT ACCESSION NO.
3. RECIPIENT'S CATALOG NUMBER	
4. TITLE *(and Subtitle)*: THE MEASUREMENT OF RESIDUAL STRESS WITH X-RAY DIFFRACTION	5. TYPE OF REPORT & PERIOD COVERED: Final Report
	6. PERFORMING ORG. REPORT NUMBER
7. AUTHOR(s): Charles P. Gazzara	8. CONTRACT OR GRANT NUMBER(s)
9. PERFORMING ORGANIZATION NAME AND ADDRESS: Army Materials and Mechanics Research Center, Watertown, Massachusetts 02172 DRXMR-OM	10. PROGRAM ELEMENT, PROJECT, TASK AREA & WORK UNIT NUMBERS: D/A Project: 1L161102AH42; AMCMS Code: 61102A
11. CONTROLLING OFFICE NAME AND ADDRESS: U. S. Army Materiel Development and Readiness Command, Alexandria, Virginia 22333	12. REPORT DATE: May 1983
	13. NUMBER OF PAGES: 45
14. MONITORING AGENCY NAME & ADDRESS*(if different from Controlling Office)*	15. SECURITY CLASS. *(of this report)*: Unclassified
	15a. DECLASSIFICATION/DOWNGRADING SCHEDULE

16. DISTRIBUTION STATEMENT *(of this Report)*

Approved for public release; distribution unlimited.

17. DISTRIBUTION STATEMENT *(of the abstract entered in Block 20, if different from Report)*

18. SUPPLEMENTARY NOTES

Much of the material presented in this report is the result of research (6.1) and Materials Testing Technology (MTT) projects conducted at AMMRC and was presented at a seminar at the Naval Air Rework Facility in San Diego, Calif. on 18 and 19 November, 1981.

19. KEY WORDS *(Continue on reverse side if necessary and identify by block number)*

Residual stress
X-ray analysis
X-ray diffraction
Nondestructive testing
Instruction manual

20. ABSTRACT *(Continue on reverse side if necessary and identify by block number)*

(SEE REVERSE SIDE)

DD FORM 1 JAN 73 1473 EDITION OF 1 NOV 65 IS OBSOLETE

UNCLASSIFIED

SECURITY CLASSIFICATION OF THIS PAGE *(When Data Entered)*

Block No. 20

ABSTRACT

A concise summary of the application of X-ray diffraction principles involved in the measurement of residual stresses is presented for those users of this technique having little exposure to this field. The latest developments in X-ray diffraction residual stress analysis, XRDRSA, are applied in simplified form so that this report can serve as a working manual.

Five general areas are considered, namely: theory, history and progress, technical problems, apparatus, and examples of specific problems involving the measurement of residual stresses using X-ray diffraction procedures.

Much of the material presented is the result of research (6.1) and Materials Testing Technology (MTT) projects conducted at AMMRC and was presented at a seminar at the Naval Air Rework Facility in San Diego, Calif. on 18 and 19 November, 1981.

CONTENTS

FOREWORD

The purpose of this report is to provide a concise, current, and simple working manual on X-ray diffraction residual stress analysis (XRDRSA). This material is directed towards the field user who has neither the manpower nor the time to commit for application of a technique that is, at present, accepted to be the most accurate means of determining residual stresses nondestructively in the surface of a crystalline material. For those laboratories, such as at AMMRC, which possess a balance of research (6.1) and the applied state-of-the-art (6.3, MTT), this report may be useful to the applications engineer and also to the technical manager, whose responsibility encompasses a rather broad scope. However, in many industrial settings and military installations, which are directed to apply the test methods in a challenging array of diversified field problems, this report will probably be most useful.

The area of XRDRSA is in a state of evolutionary flux. While much apparatus is developing rapidly, and indeed is being used in many field settings, many technical problems associated with some of these applications are under investigation and being reported in technical journals. Indeed, this points out what price is to be paid for leaving technical gaps in the development of methods, such as in the area of XRDRSA.

The need for this presentation suddenly climaxed with a technical consulting visit to the U.S. Naval Air Rework Facility, NARF, in San Diego, Calif. on 18-19 November, 1981. Essentially, most of the contents of this report were presented to a group, with broad backgrounds, at NARF. It was at the suggestion of Mr. Jeff Sakai, who painstakingly arranged the seminar, that this report be written, since the contents of which are finding their way to an interested audience in a rather loose and somewhat disjointed form.

INTRODUCTION

The format of this report will consist of five sections, namely:

(1) Theory

The theoretical background will be given in short and simplified form. In some cases the treatment of the material will only serve to "define" the terms used in the subsequent presentation.

(2) History and Progress

This section, almost always neglected in papers on this subject, may serve to afford an understanding of the present conditions in the field of XRDRSA as well as an appreciation of the attention given to particular aspects of the methods involved.

(3) Technical Problems

The primary problem areas associated with XRDRSA are with grain size, surface conditions, and texture, or preferred orientation. These problems are reviewed and examples given; illustrating the extent of these effects and how to correct for them.

(4) Apparatus

A comparison of the X-ray equipment developed and applied in measuring residual stress is given; illustrating the important features of the apparatus available.

(5) Applications

Examples of applications of XRDRSA to specific problems will be discussed along with the approach taken to avoid or solve them. It is intended that the steps taken in arriving at solutions will serve as guidelines towards a systematic, and hopefully efficient, approach to applying XRDRSA to a wide range of field problems.

THEORY[1]

The term diffraction, taken literally, means "break into pieces." From the wave theory of light, which was well established before X-rays were known to exist, light waves scattered from gratings, or lines, were known to "interfere" destructively and yield no light, while others interfered constructively and gave intense light patterns or fringes. Since gratings could be made with separation distances the same as the wavelength of light (the wavelength of light, approximately 3000 A, is roughly equal to the separation of grating spacings produced mechanically [10^{-5} in.]) light diffraction was simple to achieve.

1. CULLITY, B. D. *Elements of X-ray Diffraction,* Addison Wesley, Reading, Massachusetts, 1967, gives a more in-depth presentation of the following theory of X-ray diffraction and residual stress analysis.

Max von Laue, in 1912, with a single stroke of creativity, reasoned that X-rays have the same wavelength as the separation distances of one of the most accurate gratings available. Furthermore, these gratings are available in nature and can also make use of the penetrating power of X-rays. These gratings are the crystal lattice of crystalline materials. Thus, it became possible to obtain the first three-dimensional diffraction of "waves" or X-rays.[2] Hence, the field of X-ray diffraction, of which XRDRSA is a small segment, can be traced to this idea.

Origin of X-rays

X-rays, as electromagnetic waves, can be produced as a result of an atomic reaction or a "radiation event". The way that X-rays are created for almost all work performed in XRDRSA, is by utilizing the physical phenomenon that if an electron is given sufficient kinetic energy and is brought to a sudden stop, X-rays will be produced. Since electrons travel relatively unimpeded in a vacuum, X-ray tubes are vacuum tubes. In addition, much heat is generated at the "target," so that the target is almost always water-cooled. A "window" provides an escape path for X-rays that can be "reflected" or diffracted from a specimen, as shown in Figure 1. Similar to the case of light reflection, if the specimen is rotated at half the angular speed as that of the detector, accepting X-rays after reflection, the incident angle θ equals the diffracted angle θ.

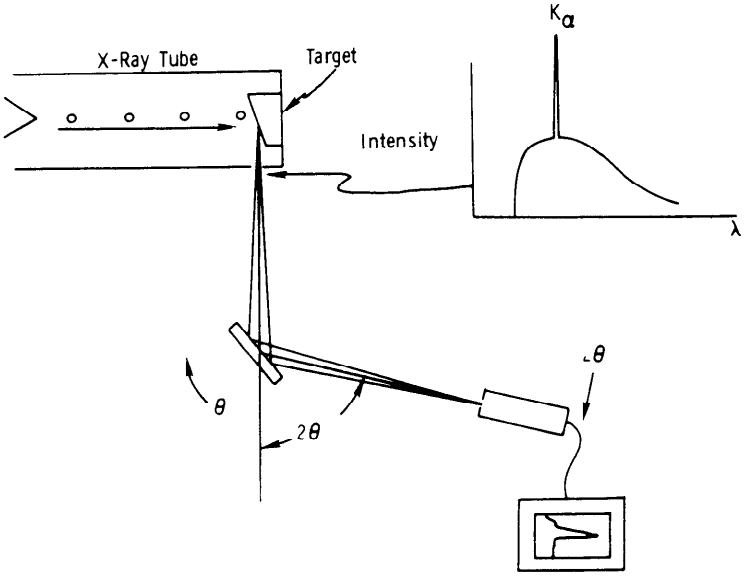

Figure 1. Schematic diagram illustrating spectrum of an X-ray tube and Bragg powder diffraction. The intensity distribution is shown as a function of the wavelength λ. The angular velocity of the specimen is given as $\omega = \dot{\theta} = d\theta/dt$ while the detector velocity is $2\theta = 2d\theta/dt$.

2. FRIEDRICH, W., KNIPPING, P., and VON LAUE, M. *Interferenz-Erscheingen bei Rontgenstrahlen,* Ber. bayer. Akad. Wiss., 1912, p. 303.

Another important property of X-rays is that in creating X-rays, if the incident electron "bumps" and removes an electron from an inner shell of a target atom, an intense characteristic X-ray beam with a wavelength peculiar to the shell type and target material is emitted. The significance of this event is that a means of creating an X-ray with a wavelength that is always the same (regardless of temperature, pressure, etc.) provides us with a standard for the XRDRSA tool. Shown in Figure 1 is a characteristic K line on top of what is termed "white radiation".

Diffraction Planes (hkl)

In order to speak of specific planar surfaces in a crystal lattice and their orientation, we use a system of indices similar to a set of "navigational" coordinates, called the Miller indices.

The coordinates employed are taken relative to a "unit cell." The unit cell is the highest symmetry unit with the smallest dimensions, which we can conveniently select to characterize the crystal structure of the material under investigation. For simplicity in demonstration, a simple cubic unit cell is shown in Figure 2. The Miller indices are defined, in Figure 2, as the inverse of the intercepts of the plane along $\bar{a}$, $\bar{b}$, and $\bar{c}$, respectively, and reduced to the smallest whole numbers. Therefore, $(\frac{3}{2},0,1)$ would reduce to (302).

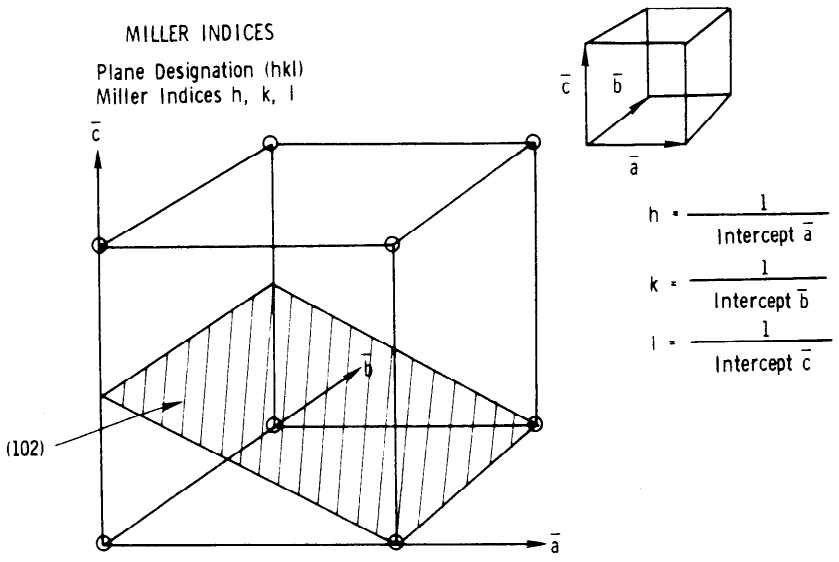

Figure 2. A graphical explanation of the Miller indices as related to a cubic unit cell.

Crystal directions are expressed by square brackets and the indices are represented by the coordinates. Hence, the vector $\bar{a}$ could be described as [100], $\bar{b}$ as [010] etc. The unit cell diagonal direction would be [111]. Curly brackets denote families of planes; i.e. {100} includes (100), (010), (001), $(\bar{1}00)$, $(0\bar{1}0)$, and $(00\bar{1})$.

Diffraction

The most important equation in X-ray diffraction is that discovered by W. L. Bragg,[3] called Bragg's Law, which is:

$$\lambda = 2\, d \sin\theta \quad , \tag{1}$$

where d is the distance between diffraction planes, Bragg's simplistic drawing of a cubic cell diffracting X-rays (note the graphical representation of the variables so that the waves can constructively interfere) bears repeating in Figure 3; in it the derivation of Bragg's Law is so nicely illustrated. Notice that the extra path-length taken by the second wave of X-rays (lower) is $2(d \sin\theta)$ and is equal to one whole wavelength (or, an integral number of wavelengths). In addition, for cubic crystals:

$$d = a/(h^2 + k^2 + l^2)^{1/2} \tag{2}$$

where a is the lattice constant.

In XRDRSA, it is assumed that diffraction occurs in a polycrystalline or "powder" material. This means that those crystals, in a polycrystalline aggregate, whose crystallographic planes are correctly oriented to diffract X-rays, each contribute a portion of X-rays to the "total" diffracted X-ray beam, as shown in Figure 4. The ideal grain size for the polycrystalline material to yield the most accurate statistics is approximately 10 - 50 μM.

Residual Stress

Residual stresses are either compressive or tensile in nature. The effect of a residual stress on the 2θ position of a Bragg reflection, or the diffracted X-ray beam position, is schematically shown in Figure 5. The initial position of the atoms (without stress, i), is seen to be reduced from d_i to a smaller separation d_f (final stress condition, f) with the application of a compressive stress. According to Bragg's Law, this corresponds to an increase in θ for the application of a compressive stress. Likewise, a tensile stress decreases the Bragg angle, θ.

3. BRAGG, W. L. *The Diffraction of Short Electromagnetic Waves by a Crystal,* Proc. Camb. Phil. Soc., v. 17, 1912, p. 43.

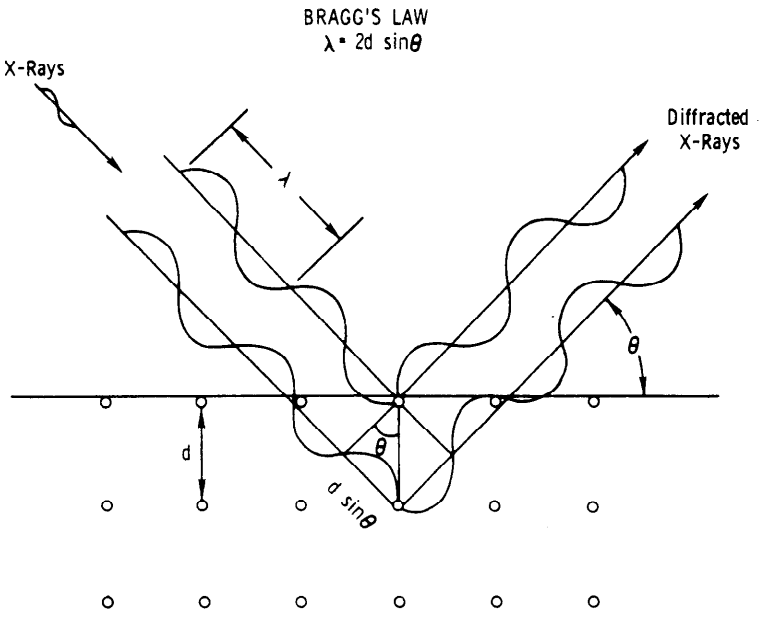

Figure 3. A simplified derivation of Bragg's Law.[3] Notice that all of the variables in Bragg's Law are illustrated.

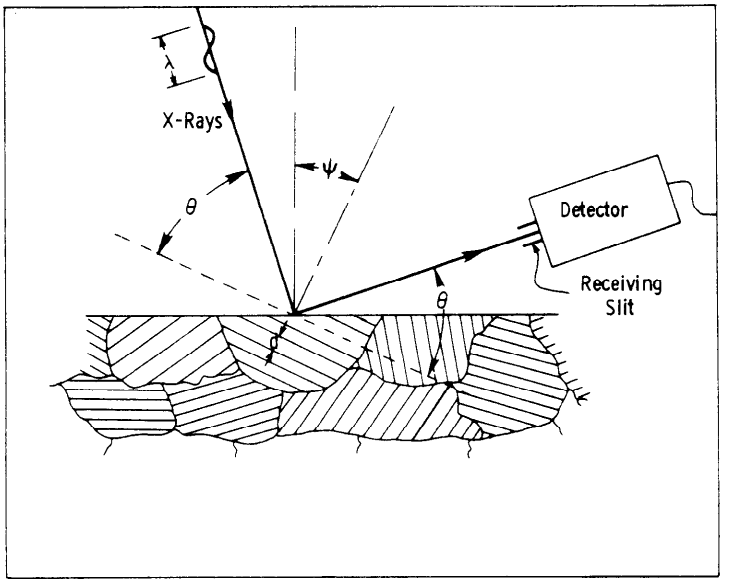

Figure 4. Schematic of atomic planes in a "grain" properly oriented for diffraction of X-rays according to Bragg's Law. Note the relationship of the inclination angle, ψ.

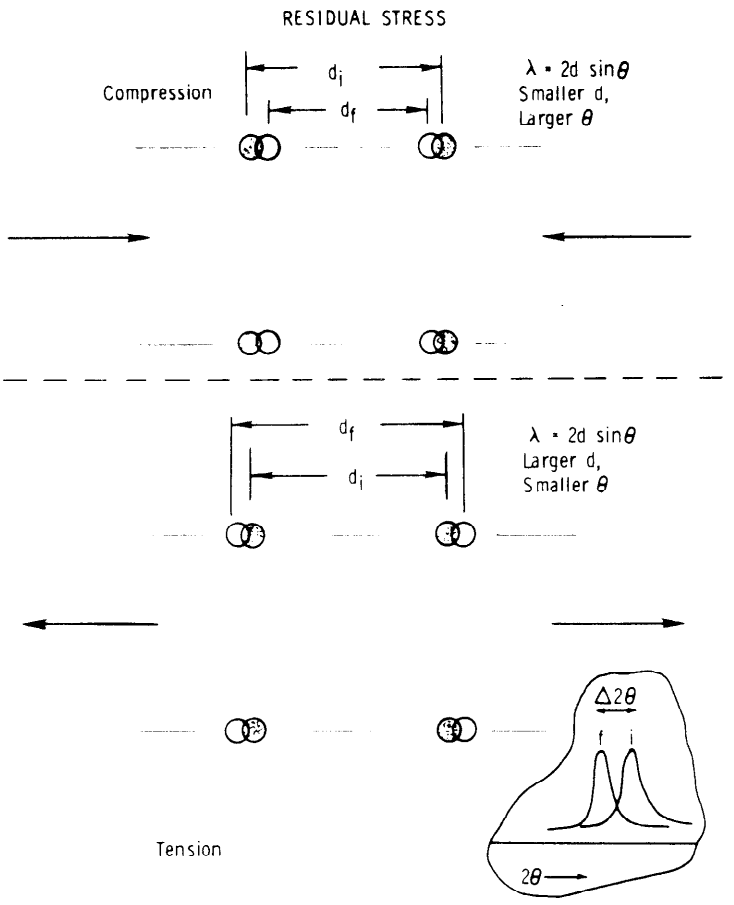

Figure 5. The effect of stress on the position of atoms and the Bragg angle, θ.

The derivation of the residual stress, σ_ϕ, in terms of the X-ray parameters is given in Reference (4). However, a simplified form of the derivation is presented, following the treatment of Cullity.[1]

In Figure 6, a stress-strain ellipsoid is shown defining the necessary terms in the derivation. It should be noted that the following treatment assumes a strictly elastic behavior of the stress with strain; hence, E, the Modulus of Elasticity and ν, Poisson's ratio, are employed. Also, strictly speaking, the elastic strain is effectively measured and converted to stress. It should also be pointed out, that the surface stress, σ_ϕ, can only be directly obtained from a single measurement, by finding d_i or d_ψ, where $i = \psi = 90^\circ$, or d is in the plane of the sheet, a physically impossible measurement to make in reflection. The strategy, then, is to obtain measurements as close to $\psi = 90^\circ$ as possible (as well as at $\psi = 0^\circ$, and at other ψ angles), in order to be able to extrapolate to the surface value of σ_ϕ.

4. *Residual Stress Measurement by X-ray Diffraction,* SAEJ784a, Soc. of Aut. Engrs. Inc., Warrendale, Pa., 1971.

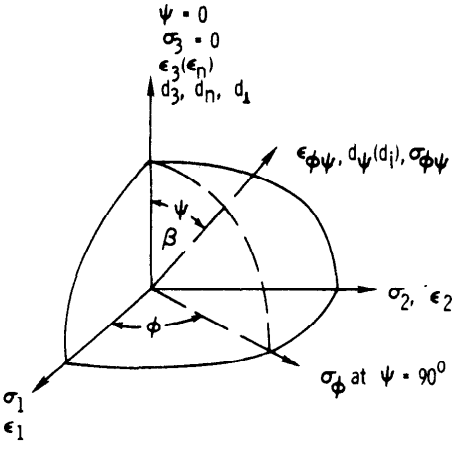

Figure 6. Stress and strain ellipsoids illustrating the parameters employed in X-ray diffraction residual stress analysis (XRDRSA).

For poles normal to the surface:

$$\varepsilon_3 = \varepsilon_z = -\frac{\nu}{E}(\sigma_1 + \sigma_2) + \frac{\sigma_3}{E} \quad , \tag{3}$$

but, $\sigma_3 = 0$, since the stress normal to the surface is zero,

$$\frac{d_n - d_o}{d_o} = \varepsilon_3 = -\frac{\nu}{E}(\sigma_1 + \sigma_2) \tag{4}$$

d_n = d-spacing for normal to diffracting plane.

Move the diffraction normal in the direction specified, by ϕ, and in the amount ψ. Now, the strain will be defined as:

$$\varepsilon_\psi = \frac{d_i - d_o}{d_o} \tag{5}$$

d_i = d-spacing in direction specified,

d_o = d-spacing without stress.

From the Theory of Elasticity:

$$\varepsilon_\psi - \varepsilon_3 = \frac{\sigma_\phi}{E} (1 + \nu) \sin^2 \psi \quad . \tag{6}$$

Substituting for these values of ε_3 and ε_ψ results in:

$$\frac{d_i - d_o}{d_o} - \frac{d_n - d_o}{d_o} = \frac{\sigma_\phi}{E} (1 + \nu) \sin^2 \psi \tag{7}$$

or

$$\boxed{\sigma_\phi = \frac{E}{(1 + \nu)} \sin^2 \psi \frac{d_i - d_n}{d_n}} \tag{8}$$

since $d_n \approx d_o$.

Differentiating Bragg's equation and dividing by λ gives:

$$\frac{\Delta\lambda}{\lambda} = \frac{2\Delta d \sin\theta + 2d \cos\theta \Delta\theta}{2d \sin\theta} = 0 \tag{9}$$

or

$$\frac{\Delta d}{d} = - \cot\theta \Delta\theta = - \frac{\cot\theta \Delta 2\theta}{2} \quad . \tag{10}$$

But, $\frac{\Delta d}{d} = \frac{d_i - d_n}{d_n}$; so Equation (8) becomes:

$$\sigma_\phi = \frac{E \cot\theta (2\theta_n - 2\theta_i)}{2 (1 + \nu) \sin^2 \psi} = K (2\theta_n - 2\theta_i) = K\, 2 \Delta \theta \quad . \tag{11}$$

Since diffracting conditions are not perfect, or a systematic alignment error is usually present, the $2 \Delta \theta$ of a standard or stress-free sample of a similar

material is measured to correct for this effect. Therefore, a corrected version of the final equation is:

$$\sigma_\phi = K\ (2\ \Delta\ \theta_{specimen} - 2\ \Delta\ \theta_{standard}) \quad . \tag{12}$$

The important consequence of this equation is that σ_ϕ is linear in $\sin^2\psi$. This assumption is utilized in employing the two ψ method shown in Figure 7. Measuring 2θ at $\psi = 0$ and at $\psi = 45^\circ$ allows one to extrapolate to σ_ϕ at $\psi = 90^\circ$.

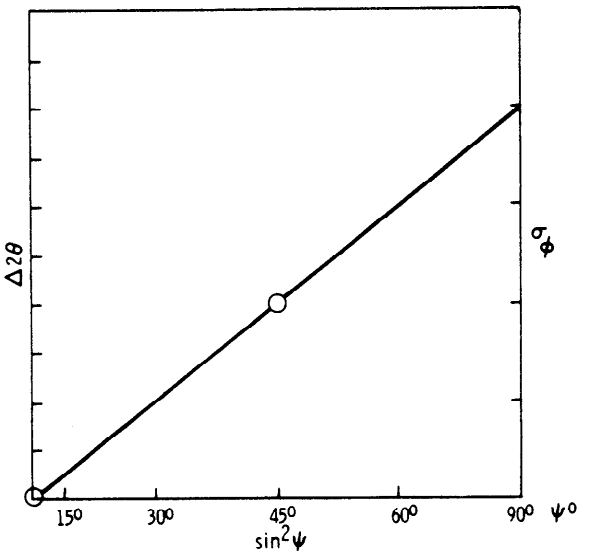

Figure 7. A graphical method of extrapolating to the surface residual stress with shifts in Bragg angles at $\psi = 0$ and 45°, Glocker method. (σ_θ must be linear with $\sin^2\psi$).

A working graph for the (211) reflection of α - iron (or martensitic steel) is shown in Figure 8, utilizing CrKα X-radiation. In this case, measurements can be made at $\psi = 15^\circ$, 30°, and 60° to establish a better linear fit.

A final word should be given concerning the units employed for σ_ϕ. Since E, in the cgs system, is given in dynes/cm^2, and in the English system in psi:

1 dyne (dyn) = a force of 0.00102 gms, and since 1 dyn = (0.00102) (980.665 cm/sec^2)

1 Newton (N) = 10^5 dyn.

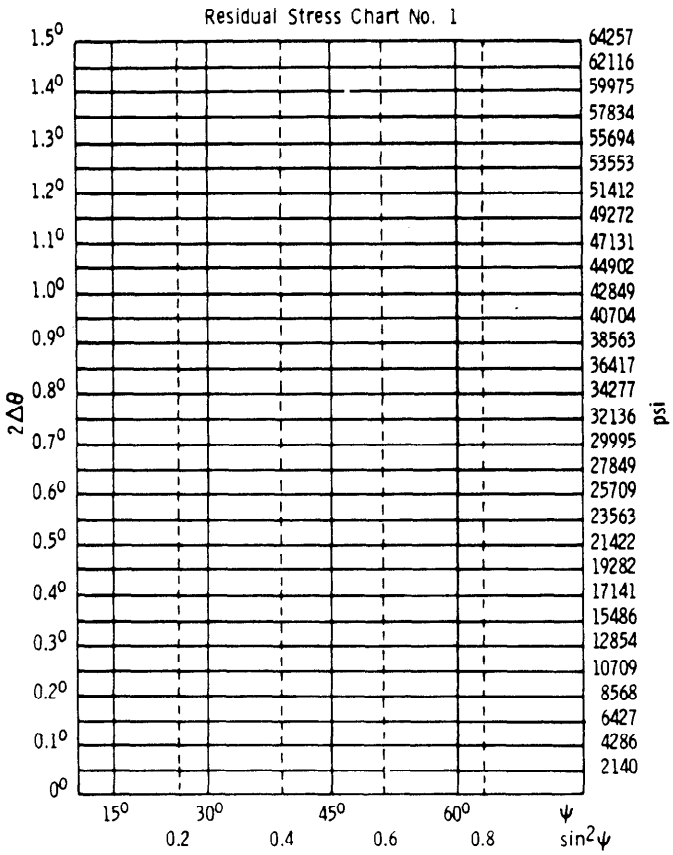

Figure 8. A $\Delta 2\theta$ vs $\sin^2 \psi$ graph developed for carbon steel (α') facilitating extrapolation of σ_θ.

Now, 1 Pascal (Pa) = 1 N/m^2 = 10 dyn/cm^2 = 1.45038 x 10^{-4} psi

1 M Pa = 0.145038 ksi or 6.8947 M Pa = 1 ksi (where M = 10^6)

1 M Pa = 145.038 psi or 0.0068947 M Pa = 1 psi .

X-ray Safety

For most applications of X-ray diffraction, harmful X-rays can be automatically shielded or removed to protect the operator. However, in the case of XRDRSA, most cases include a variety of specimens of different shapes and sizes, or the diffractometer is taken to the specimen without essentially changing its shape or physical condition. This presents an additional hazard in radiation protection. Effectively, this means that radiation surveys should be performed for each physical configuration of a specimen examined, and the necessary precautions employed. For example, once the specimen has been placed relative to the X-ray diffractometer, a survey meter, that is sensitive to X-rays, will be used to measure X-rays scattered in "all directions," particularly in the backscattered direction. Proper shielding will be so placed in order to protect the operator, and surveying should be repeated, with the shielding in place, prior to taking measurements for XRDRSA.

HISTORY AND PROGRESS

In presenting any historical review, the greatest danger is that of omitting a particular effort made by some noteworthy researcher. In this spirit, it is hoped that the reader consider that the contents reflect the writer's perception and exposure to the development of the field of XRDRSA.

The beginning and keystone of any work in the X-ray area began with the discovery of X-rays by W. C. Roentgen in 1895. In addition, it is known that Roentgen even attempted to reflect X-rays from a calcite crystal but failed, due to his underestimation of the intensity of the reflected beam.

A chronological series of events, illustrating the milestones in the development of XRDRSA, is shown in Figure 9.

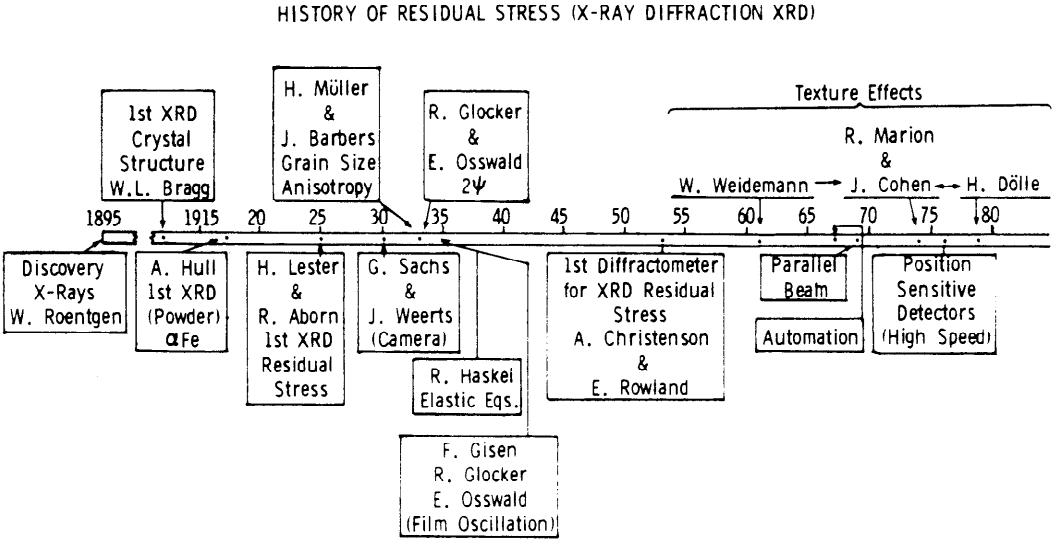

Figure 9. A chronological chart depicting some historical milestones in the evolution of XRDRSA.

The first crystal structure determination performed, along with the discovery of Bragg's Law, was in 1912, and resulted in the presentation of the Nobel prize to Bragg.[3]

A. Hull,[5] working in the U.S.A. in 1917, and P. Debye and P. Sherrer[6] in Europe in 1916, with independent efforts, were the first to use a powder to obtain a diffraction pattern. Hull performed the first powder pattern crystal structure determination of α-iron.

5. HULL, A. W. *The Crystal Structure of Iron,* Phys. Rev., v. 9, 1917, p. 84.
6. DEBYE, P., and SHERRER, P. *Interferenz an regellos orientierten Tielchen im Rontgenlicht I.,* Phys. Zeits., v. 17, 1916, p. 277.

The beginning of XRDRSA is documented with the work of H. Lester and R. Aborn[7] at the Watertown Arsenal, Watertown, Mass. In 1925, a powder camera and an X-ray generator were constructed (see Figure 10), and residual stress calculations were made from single-strain measurements conducted at $\psi = 0^{o}$. Also shown in Figure 10, is a Sachs-Weerts residual stress camera that was commonly used in the early 30's. At the same arsenal, in 1934, R. K. Haskel[8] developed the elastic equations in a form that could be applied to XRDRSA. In the same year, R. Glocker and E. Osswald[9] were able to make a great breakthrough in determining the residual stress vector σ_{ϕ} using two strain measurements at $\psi = 0^{o}$ and at $\psi = 45^{o}$, assuming a linear dependence on $\sin^2 \psi$. This method was used almost exclusively until the middle 70's and has come to be known as the "Glocker Method".

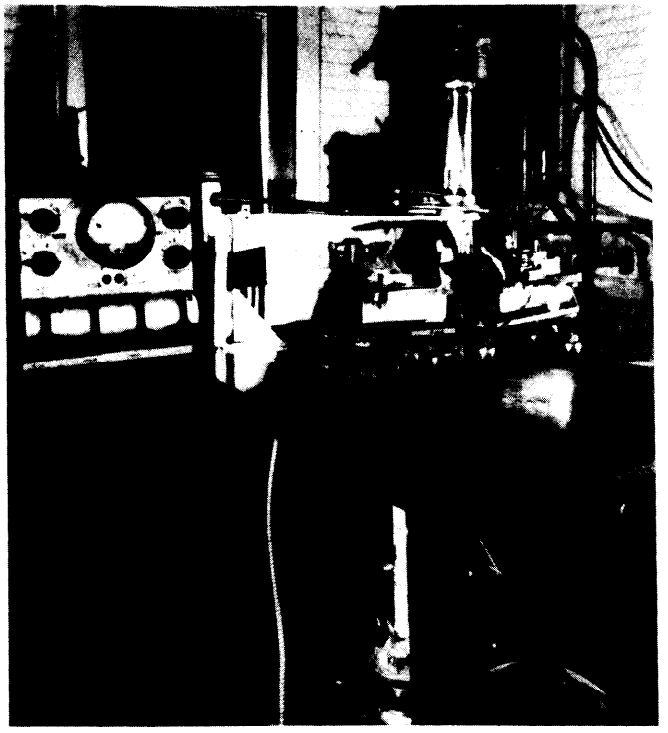

Figure 10. "Where it Began". First X-ray diffraction system at Watertown Arsenal (H. H. Lester) shown with G. Sachs–J. Weerts residual stress camera (circa 1933).

7. LESTER, H. H., and ABORN, R. H. *Behavior Under Stress of the Iron Crystals,* Army Ordnance, v. 6, 1925, 1926, pp. 120, 200, 283, 364.
8. HASKEL, R. K. *X-ray Diffraction as Applied to the Determination of Stress Conditions in Gun Steel,* Watertown Arsenal Rpt. No. 160/2, Watertown, Mass., 1934.
9. GLOCKER, R., and OSSWALD, E. *Unique Determination of the Principal Stresses with X-rays,* Z. Tech. Physik, v. 161, 1935, p. 237.

Evidence that 1934 was a productive year in XRDRSA, and that many ideas that have been thought of as originating in recent years may indeed not be, H. Moller and J. Barbers[10] concluded, "The grains are not taking up strain homogeneously", and that, "There are different physical properties in different directions; anisotropy exists in the grain boundries and grain size can give erroneous residual stresses". These statements made 48 years ago are timely today in XRDRSA and yet occupy the attention of research workers.

Since then, and extending through the time of WWII, efforts in improving methods in XRDRSA were minimal, until in 1953, A. Christenson and E. Rowland[11] introduced the XRD goniometer, or diffractometer, to residual stress analysis. This eliminated the necessity for cameras and film, allowing for direct quantification of the X-ray lines and, therefore, speeded up measurements from hours to minutes. It now became possible for a two-exposure XRDRSA to be performed in approximately 20 min on steel.

A German researcher, in work done on his thesis, was able to give great insight to a problem plaguing the XRDRSA community, that of a texture effect. In 1961, W. Weidemann,[12] was able to explain a phenomenon in the creation of texture, or preferred orientation, in which he described two classes of crystallites; those deformed plastically and those elastically loaded that contribute to a texture-related shift in the diffraction line. This operation will be discussed in the next section.

A breakthrough in reducing the time for making an X-ray stress measurement, was made in 1967 with the introduction of the "Fastress* X-ray System", whereby two X-ray tubes and detector systems made measurements simultaneously at two ψ angles, with a subsequent computerized calculation of the residual stress in approximately two minutes.

In Japan, in the late 60's, an effort was underway to measure residual strains with an emphasis on parallel beam optics rather than the customary divergent beam geometry employed in XRDRSA. The chief advantage with parallel beam optics, is that the error introduced with the positioning of the specimen, with divergent beam focussing, is reduced by a factor of approximately ten times with a parallel beam system.

In the mid 70's, research on the texture problem was directed by J. Cohen of Northwestern University and yielded a correction procedure for texture effects on XRDRSA, based on the work of Weidemann. This procedure came to be known as the

*Developed at General Motors Technical Center, Warren, Mich., produced by American Analytical Corp.

10. MOLLER, H., and BARBERS, J. *X-ray Investigation of the Stress Distribution and Overstraining in Ingot Steel,* Mitt. Kaiser-Wilhelm-Inst., EisenForsch, Dusseldorf, v. 16, 1934, p. 21.
11. CHRISTENSON, A., and ROWLAND, E. *X-ray Measurement of Residual Stress in Hardened High Carbon Steel,* Trans. Am. Soc. Metals, v. 45, 1953, p. 638.
12. WEIDEMANN, W. *PhD. Thesis,* Technische Hochschule, Aschen, Germany, 1966, synopsis in Reference 13. Also published with BOLLENROTH, V. F., and HAUK, V. *Zur Dentung der Gittereigenverformungen in Plastich Verformtem-Eisen,* Arch. fur Eisen, v. 10, 1967, p. 793.

Marion-Cohen method.[13] Recently, H. Dolle,[14] in a generalized treatment of this problem, has essentially theoretically solved the case of elastic anisotropy and texture in XRDRSA (1979). Cohen helped Dolle in applying these results[15] and hopefully the problem of texture may soon be solved with the production of substantiating data.

The 70's was also a time for advances in X-ray equipment, especially with the application of position sensitive detectors (PSD). It is now possible to make measurements in times down to 15 sec with such computerized systems.

The 80's may see further application of PSDs, but also the increase in X-ray flux with rotating anode X-ray tubes, accelerators, etc. High energy X-ray systems are being introduced to measure stresses deeper into materials and also in transmission.[16]

Finer resolution of detectors is opening up opportunities for energy dispersive applications in XRDRSA and some interesting possibilities are being considered for a variety of applications.

The accuracy of XRDRSA, for the case of steel, (α-iron), has progressed from roughly double-digit ksi in the 30's, to about 5 ksi in the 50's, to approximately 2 ksi at present. This level will not change substantially. What is more significant is that the difficulty lies in making it possible for the many users of XRDRSA to achieve the accuracies already available with the current state-of-the-art procedures.

TECHNICAL PROBLEMS

The XRDRSA method has many advantages over other techniques at the present time. However, there are also disadvantages, some of which can be eliminated or allowed for, following special procedures. A summary of these advantages and disadvantages are listed in Table 1. For an in-depth treatment of these problems the reader is referred to References (6) and (17).

The subject of this section is those problems listed that can be experimentally dealt with or corrected. The main problems can be broadly grouped into three areas, namely; texture, grain size, and surface effects, or distortion. These effects on the $\Delta\ 2\theta$ vs $\sin^2\ \psi$ linear plot is shown in Figure 11 and will be dealt with separately.

13. MARION, R. H., and COHEN, J. B. *Anomalies in Measurement of Residual Stress by X-ray Diffraction,* Adv. X-ray Anal., v. 18, 1975, p. 466.
14. DÖLLE, H. *The Influence of Multiaxial Stress States, Stress Gradients, and Elastic Anisotropy on the Evaluation of Residual Stresses by X-rays,* J. Appl. Cryst., v. 12, 1979, p. 489.
15. DÖLLE, H., and COHEN, J. B. *Evaluation of Residual Stresses in Textured Cubic Metals,* Met. Trans. A., v. 11A, 1980, p. 831.
16. BECHTOLDT, C. J., PLACIOUS, R. C., BOETTINGER, W. J., and KURIYAMA, M. *X-ray Residual Stress Mapping in Industrial Materials by Energy Dispersive Diffractometry,* Adv. X-ray Anal., v. 25, 1982.
17. RUUD, C. O. *Review and Evaluation of Nondestructive Methods for Residual Stress Measurement,* Elec. Pwr. Res. Inst. Rpt. NP-1971, Proj. 1395-5, September, 1981.

Table 1. ADVANTAGES AND DISADVANTAGES OF X-RAY DIFFRACTION RESIDUAL STRESS METHOD

Advantages	Disadvantages
1. Nondestructive	1. Safety hazard - X-ray and high voltage
2. Can determine stress directly from specimen (no unstressed condition necessary)	2. Low penetration into material (up to ~0.001 in. for most materials). Susceptibility to surface coatings
3. Ability to reuse, equipment unchanged	3. Condition of surface critical (i.e., machined, polished, etc.)
4. X-ray wavelength constant	4. Shape of material important (i.e., gear tooth root, rough surface, etc.)
5. Flexibility of varying λ, d, focussing conditions, etc.	5. Expensive equipment required
6. Potential for high-speed measurements (seconds)	6. Sensitive equipment required
7. Only available nondestructive practical method	7. Experimental conditions must be varied for different materials (i.e., tube change for changing λ, count speed, etc.)
8. Ability to measure stresses along steep stress gradients. Can sample small areas of specimen	8. Many complex materials parameters to be controlled (some not characterized yet): a. preferred orientation or texture b. grain size c. strain broadening of diffraction peak d. stacking faults, 2nd phase effects, etc. e. focussing system variations (i.e., divergent beam point focus vs parallel beam)
	9. Differences between mechanical and X-ray stresses (i.e., elastic constants different, etc.)

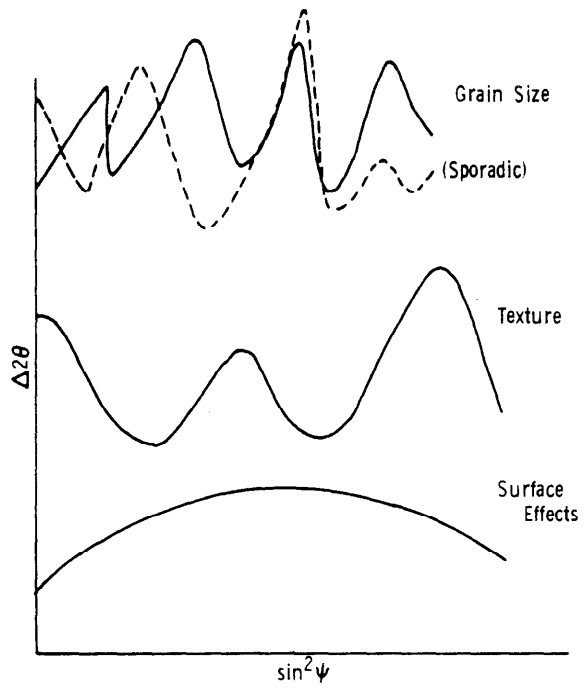

Figure 11. The effect of grain size, texture, and surface distortion on the $\Delta 2\theta$ vs $\sin^2 \psi$ curves.

Texture

A recent treatment and review of the effects of texture, or preferred orientation, on the X-ray residual stress[18] is summarized here.

To help understand the supposition made by Weidermann, and that was applied by Marion and Cohen[13] in the texture correction procedure bearing their name, we imagine a roller passing over a sheet containing two types of crystallites, A and B (see Figure 12). The A crystallites are most favorably oriented for maximum slip or plastic deformation to occur, while the B regions are not. The B crystallites do, however, undergo elastic compression during the rolling operation. Upon release of the applied load, the B regions remain under elastic compression and, hence, have a minimum d spacing relative to the A region. Therefore, d_{max} characterizes the A region and d_{min} the B region, which bound the distribution of d spacings in the rolled sheet.

The equation relating the change in d spacing, due to texture, to σ_ϕ is:

$$d_\psi - d_\perp = (d_{max} - d_B)\ f\ (\alpha,\beta) + d_B \quad . \tag{13}$$

18. GAZZARA, C. P. *The Measurement of X-ray Residual Stress in Textured Cubic Materials,* Proc. Fall Mtg. SESA, Keystone, Colo., 11-14 October 1981, p. 32.

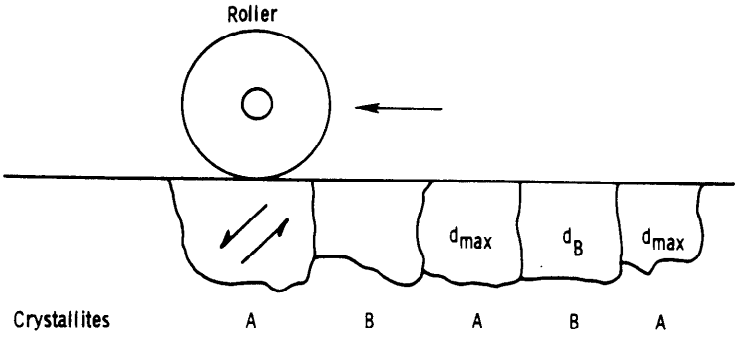

Figure 12. A graphical sequence of the steps showing the effect of texture deformation (plastic) and the elastic process on the d spacings according to Weidemann.[12]

Marion and Cohen incorporated this equation with the equation for macrostrain, so that the sum of both equations is:

$$(d_\psi - d_\perp)_{Total} = (d_{max} - d_B)\ f\ (0,\psi) + d\left(\frac{1+\nu}{E}\right)\sigma_\phi\ \sin^2\psi + d_B \quad . \qquad (14)$$

The f term gives the distribution of those crystallites (fortunately these are proportional, in number, to the diffracted intensity) whose poles align with the diffraction vector employed in the measurement (i.e., [211] for α - iron with CrKα X-radiation). The variation of an idealized f function is shown in Figure 13, as a function of $\sin^2\psi$. The associated d spacing follows the f function and, as expected, the Bragg angle, θ, is inversely related to d and f. Over the small angular range considered, $\sin\theta \approx \theta$, so that one need only consider changes in θ or $\Delta\theta$ or $\Delta 2\theta$. Also, the f function can be approximated by the diffracted peak height, h, if the width of the diffraction peak does not change appreciably with $\sin^2\psi$. For the Marion-Cohen procedure to be effective, the θ or 2θ diffraction peak curve vs $\sin^2\psi$, or vs ψ, should be exactly out-of-phase with the f or h curve. To illustrate the care that must be taken in applying this correction, curves plotted for a highly-textured heat-treated 4340 plate are shown in Figure 14. The data was taken with a Rigaku Strainflex unit, in which a parallel beam of X-rays is employed. The curves are out-of-phase by approximately 5° in ψ (ψ_o' is the observed inclination angle in the Rigaku Strainflex). Also, $\psi = \psi_o' + \eta$: where $\eta = 90 - \theta^\circ$; provided the goniometer and the specimen geometries are in alignment. In changing from a parallel beam (and fixed specimen) to a divergent beam geometry, with a Diano X-ray system, results in Figure 15, where this texture effect is shown to be minimized.

If the data, plotted in Figure 14, is corrected by the Marion-Cohen method, the σ_ϕ values (computed) include great errors and the σ_ϕ curve is shown to oscillate above and below $\sigma_\phi = 0$ (see Figure 16). Defocussing corrections are ineffective in reducing the error significantly. However, forcing the 2θ and h curves into alignment reduces σ_ϕ to 0, at high ψ values. (The specimen was unstressed, so that no residual stress should be evident.) Dolle[14] and Dolle and J. Cohen,[15] suggest employing {h00} or {hhh} reflections to eliminate the texture effect in σ_ϕ. Similar

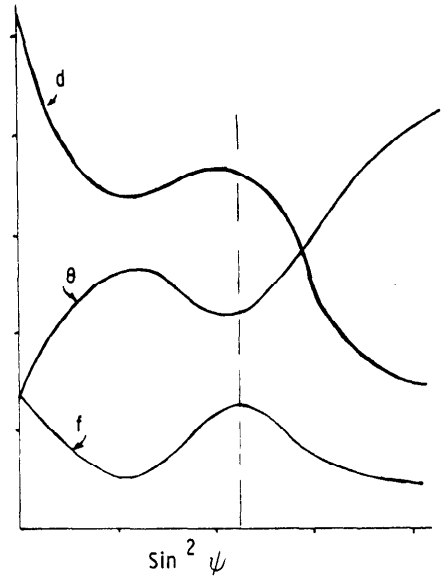

Figure 13. The idealized effects of d-spacing, θ, and f, as a function of $\sin^2 \psi$, due to texture, according to R. Marion and J. Cohen[13].

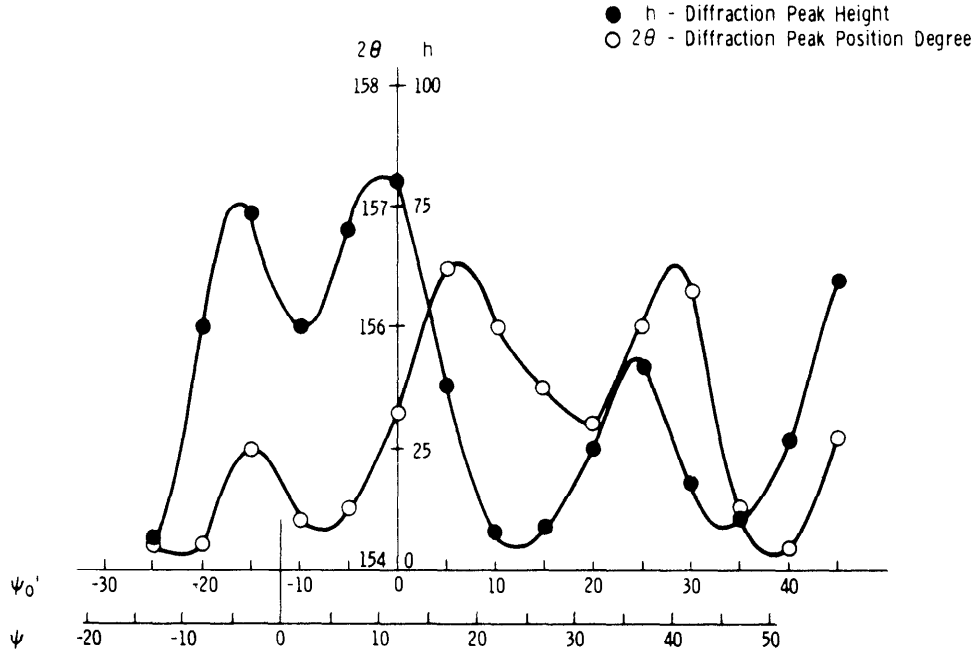

Figure 14. Bragg angle (2θ) and height (h) of the CrKα (211) diffraction peak vs ψ for a textured steel specimen (4340) using parallel beam optics (Rigaku Strainflex).

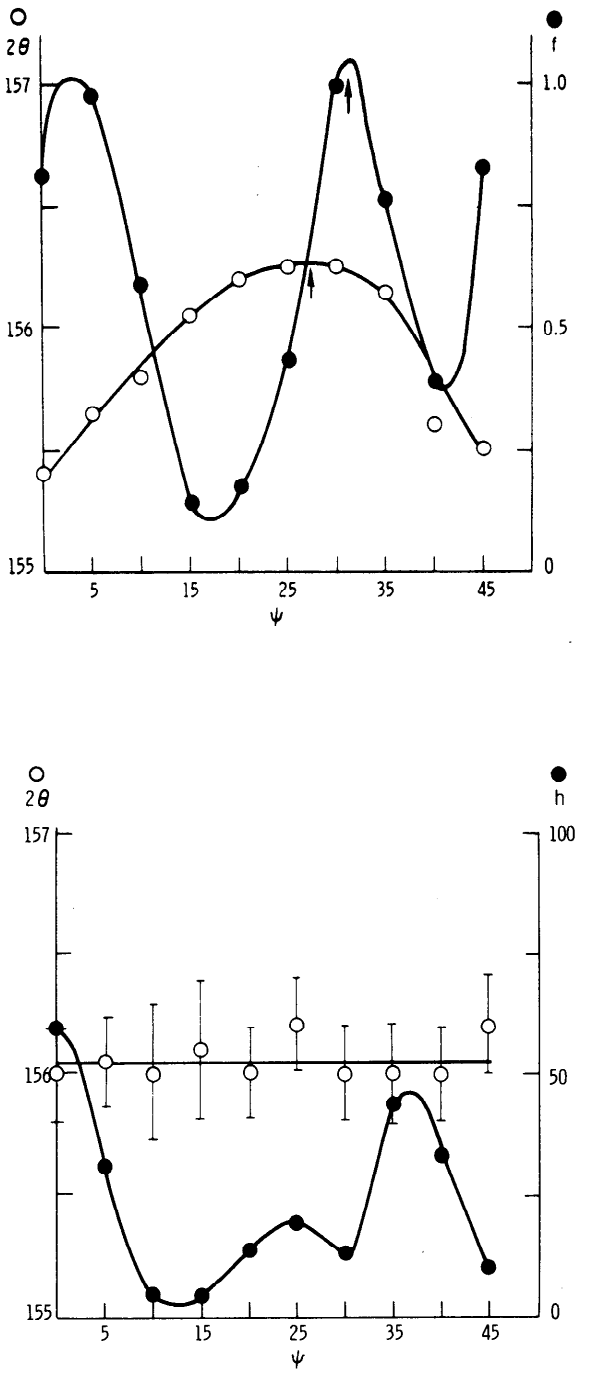

Figure 15. Bragg angle (2θ) and height (h) of the CrKα (211) diffraction peak vs ψ for 2 textured steel specimens with divergent beam optics (Diano).

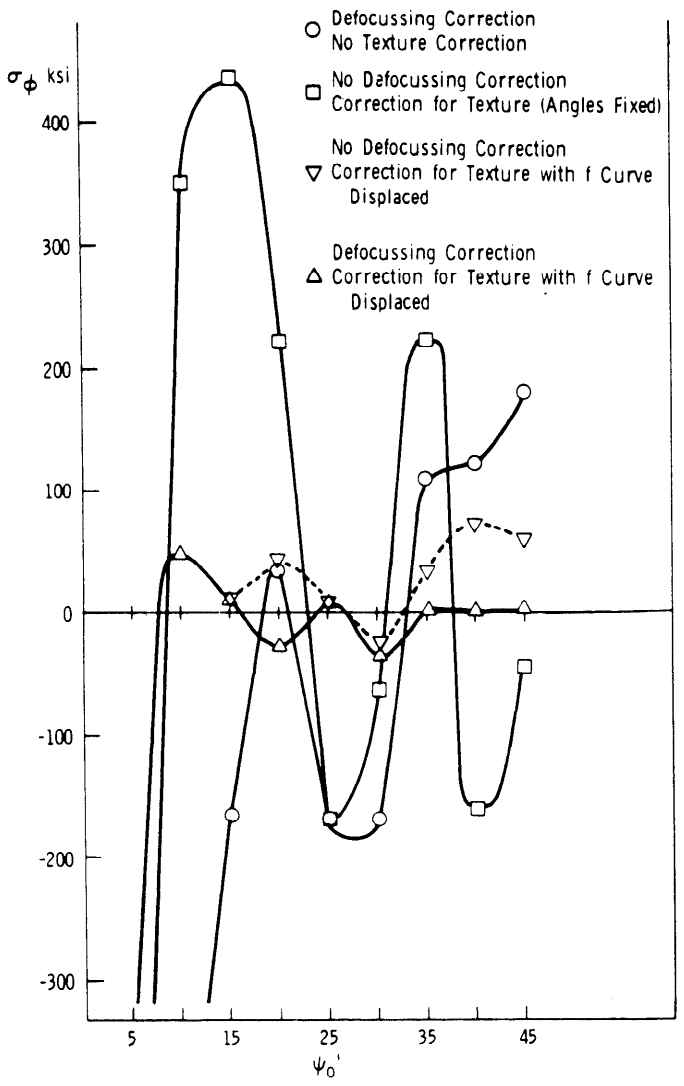

Figure 16. The effect of the angular displacement of the 2θ and h curves, in Figure 14, on the Marion–Cohen texture correction of σ, as a function of ψ_o'.

2θ and h vs ψ_o' curves are shown, using the (222) reflection, for a highly-textured aluminum alloy. As Figure 17 shows, the 2θ curve bears no relationship to the h curve, confirming these results. Another suggestion by the same authors is that the inclination angular direction be made to follow a texture independent path. (This can be determined by observing a pole figure.) This is true for the CoKα (310) reflection in α-Fe (steel), as an example. Other suggestions to minimize the effects due to texture include the application of the nondispersive technique (energy dispersive) involving the averaging of many (hkl)'s at high 2θ values.

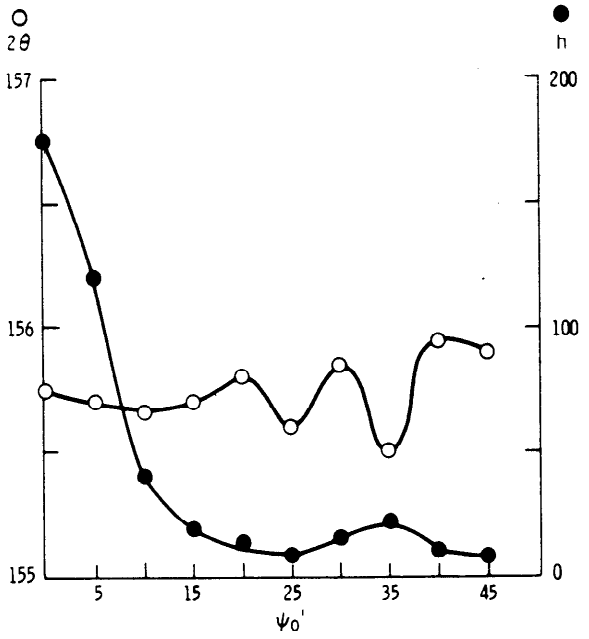

Figure 17. 2θ and h (CrKα (222) vs ψ_o' for an aluminum textured alloy specimen (ψ_o' in rolling direction).

Grain Size

The effect of grain size on σ_ϕ has been considered since the early 30's, with the use of oscillation cameras with moving cassettes, to present day equipment that oscillates the entire X-ray goniometer, such as with the Rigaku Strainflex. Aluminum alloys appear to present the greatest problem with grain size, as can be seen in Figure 17, with the variation in the diffraction peak position with inclination angle.

The grain size problem may be so severe as to tax some X-ray systems to the limit. Table 2 gives a comparison for compression aluminum standard bars[19] (see Figure 18) of calculated stresses (Column 1) and those measured with strain gauges (Column 2) with measured values of σ_ϕ, oscillating the X-ray head $\pm 3^o$ (Column 3), and $\pm 7^o$ (Column 4). These values show relatively good agreement. A system without such provisions for grain averaging, made it impossible to record any meaningful measurements (Column 5). The 7005 alloy had grains up to 1/2 mm long.

Effective solutions for large-grained specimens also include increasing the divergence of the X-ray beam, or increasing the area of X-radiation by either increasing the beam size or oscillating the specimen along the diffracting plane.

19. HORNUNG, N. L. *X-ray Stress Analysis Development of Aluminum Standards,* Spec. AMMRC Tech. Rpt. (in print).

Table 2. RESIDUAL STRESS VALUES (KSI) OF ALUMINUM ALLOY BARS

Alloy 2024 T3 - 0.090" Thickness

Bar Position	Theoretical Stress	Stress (Strain Gauge)	Rigaku(222)CrKα X-Ray ±3° Oscill TC=1 Sec (Auto Mode)	Rigaku(222)CrKα X-Ray ±7° Oscill TC=10 Sec (Graph)	DRI 333/511 CuKα
4	7.0	5.6	6.9 (11) σ=±1.7*	9.0	10.0
7	4.5	3.4	7.1 (7) σ=±1.4	6.0	(Scatter Too Large)
10	1.9	1.1	3.0 σ=±1.2	3.0	3.0

Alloy 7005 (750°F, 3 Hours, Furnace Cool) 0.250" Thickness

		(Graph)	(Graph)
4	15.7	13±2†	14±2
7	9.6	10±2	9±2
10	3.5	5±2	5±1.5

*σ = Standard Deviation. Based on Number of Measurements (11) of S.D. Residual Stress.

†Error in Residual Stress Based on Uncertainty of Diffraction Peak Position Only.

Surface Distortion

The distortion of the surface of the material can affect the stress profile to a degree that is significant for meaningful stress analysis. Results of grinding studies show[20] that gentle grinding, with oil cooling, can affect hardened steel to a 1 mil depth, conventional grinding to 3 mils, and dry, abusive grinding to 7 mils. Some researchers claim disturbed surfaces to even greater depths.

It is well-known that an electropolishing or chemical polishing treatment should be applied before X-ray residual stress measurements are made. As with most applications, particularly in the case where NDT is performed for quality control, the chemical or electropolish is too destructive and when examining steel, sometimes dangerous. (A perchloric solution is the electrolyte of choice, but is explosive.)

The procedure that has been followed at AMMRC is to make X-ray measurements before and after chemical/electropolishing to determine if the measurements before surface removal could be correlated with those after surface treatment, (assuming

20. LETNER, H. R. *Influence of Grinding Fluids Upon Residual Stresses in Hardened Steel,* ASME Trans., v. 79, 1957, p. 149.

(a)

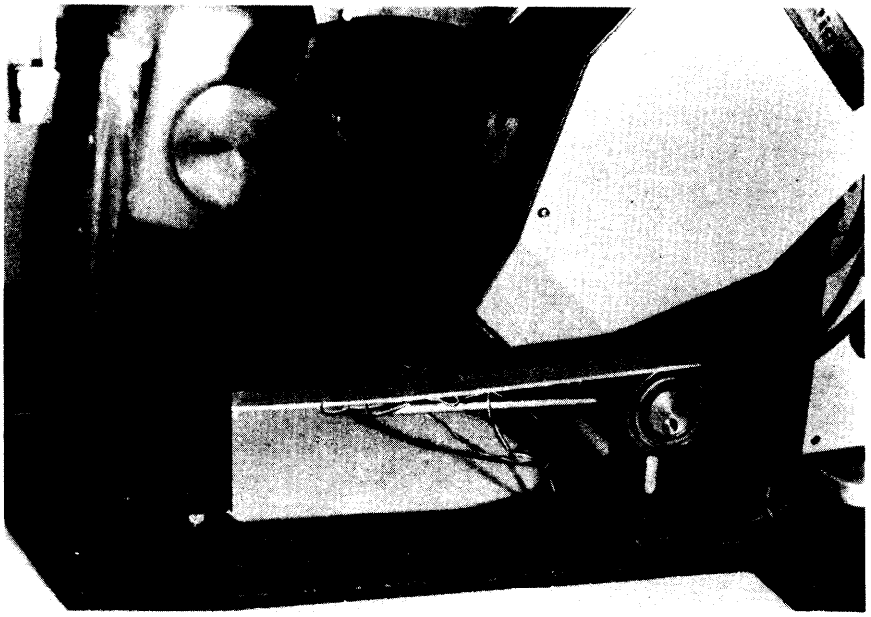

(b)

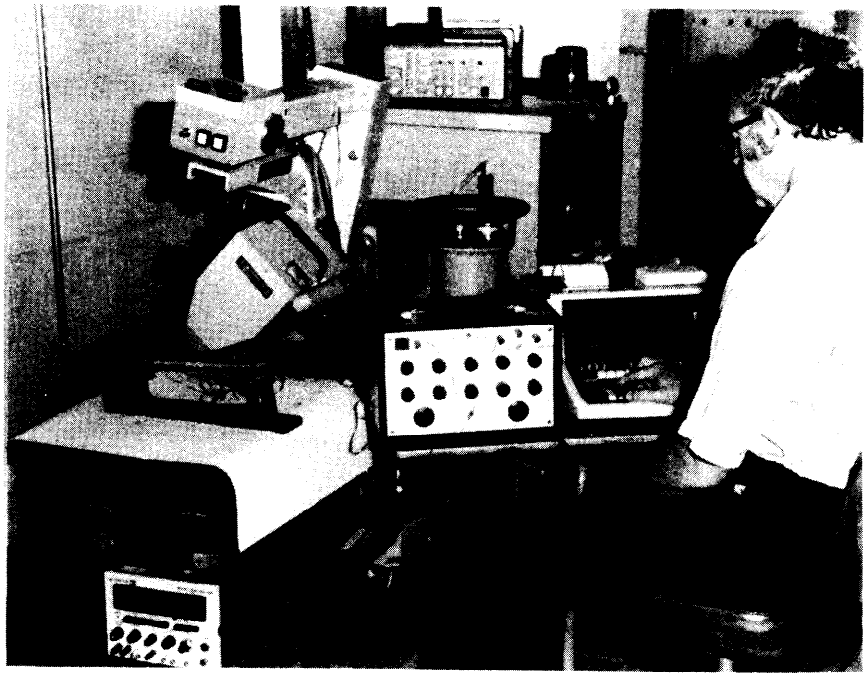

Figure 18. X-ray residual stress measurements from an elastically bent aluminum alloy calibration bar (data shown in Table 2). Notice the strain gauge test arrangement for simultaneous X-ray and mechanical stress measurements.

that the surface preparation conditions, i.e., machining, grinding, etc., have not changed). An example illustrating the importance of proper surface treatment is that of a residual stress analysis performed on an MBTA steel axle, (see Figure 19). The axle is given a thermal quench to create a surface layer in compressive stress. Residual stresses (longitudinal), at the center of the axle, before and after removal of 0.005 in. with etching, show an apparent change in stress from a compressive to a tensile mode. Subsequent residual stress measurements of this axle, using the hole-boring technique, substantiated the X-ray analysis before etching, with little change measured at a 0.005 in. deeper level. This illustrates the importance of the surface preparation, in that the etch employed, in this case, relieved the surface of the axle of residual stress. But, in the X-ray case, a decrease in compressive stress at one point does reveal a potential trouble spot, in both the as-received and etched condition. This indicates a potential quality-control application in the as-received condition even with the use of a "soft" radiation (CrKα).

One alternative to chemical or electropolishing is mechanical polishing. A technique developed at AMMRC[21] makes use of a vibratory polishing sequence that leaves the surface free from cold work. This was shown to be true for the cases of titanium alloys that are highly sensitive to cold work, in that phase transformations are easily produced. Indeed, a metastable titanium alloy (transage Ti 129) that undergoes strain induced martensitic transformation (α '') at very low strains (at approximately a 5% reduction, the transformation has been observed to occur) has been prevented using the previously mentioned polishing procedure.[22]

This technique has been applied to a steel standard on all six faces of an orthorhombic specimen and on all specimens that can be accomodated in the metallographic polishing equipment. The application of this method has become extremely valuable for residual stress analysis, but unfortunately can only be employed in limited cases due to the geometry of the specimens. Perhaps a portable vibratory polisher can be developed in cases where chemical or electropolishing equipment cannot be effectively employed.

A less-successful situation occurs, particularly on painted surfaces and in field applications. In these cases, the surface may reveal disturbed conditions with the need for surface removal, a rather difficult and destructive prospect. This points out the need for improved X-ray techniques, such as the use of "harder" (deeper) penetrating radiation.

The selection of the proper wavelength of X-radiation in XRDRSA is governed by several factors, such as: (a) the availability of an (hkl) reflection with suitable intensity at high 2θ value, (b) sufficient transmission of X-rays to reduce surface effects and grain size problems, (c) the ability to manufacture X-ray tubes with required target materials, (d) the selection of an (hkl) reflection with a high multiplicity (reduces the effects of texture or anisotropy), and far removed from neighboring diffraction peaks, and (e) results in a minimum amount of fluorescence of the sample. Curves indicating the effective diffraction depth in particular

21. FOPIANO, P. J., and ZANI, A. J. *Metallographic Preparation of Two-Phase Titanium Alloys for Replica Electron Microscopy,* Metallography, v. 3, 1970, p. 209.
22. MIDDLETON, R. M., and HICKEY, C. F. *Transformation Characteristics of Transage Ti 129,* Titanium and Titanium Alloys-Scientific and Technological Aspects, J. C. WILLIAMS and A. F. BELOV, eds., Plenum Press, N.Y., 1981.

(a)

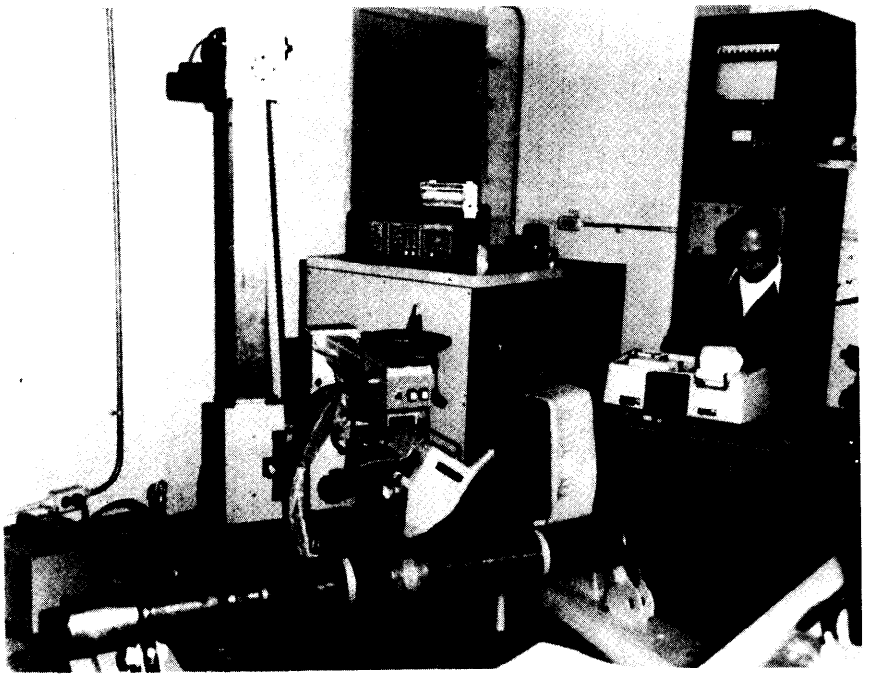

(b)

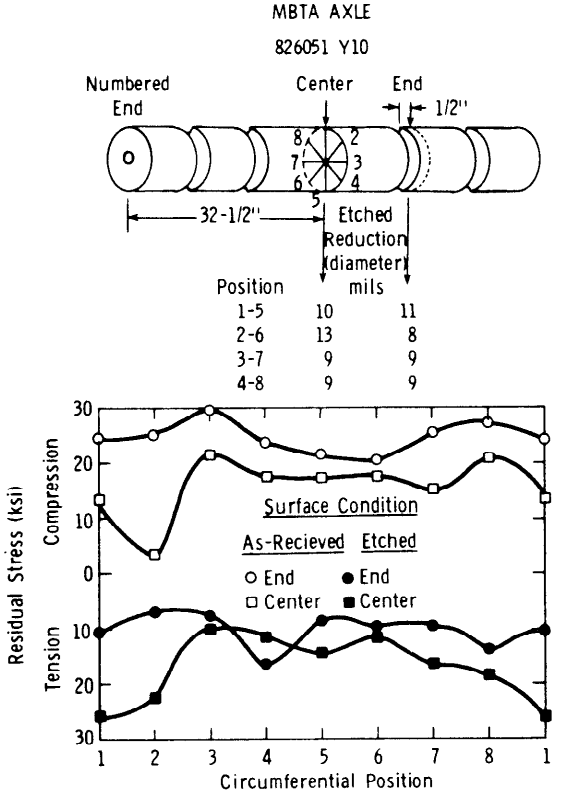

Figure 19. Residual stress measurements (longitudinal) using a Strainflex automatic (ψ_o' = 0, 15, 30, 45°) on an MBTA steel axle, before and after surface etch.

specimen elements, are shown as a function of X-ray wavelength. The Kα wavelength positions are shown at the top of Figures 20 and 21 for various target materials commonly used. Table 3 gives a listing of K lines that have been used for various materials. In each box are listed the (hkl) plane of the material and the 2θ position associated with these conditions.

A summary of the problems commonly observed in XRDRSA, with tips for their diagnosis as well as some proposed solutions, is given in the work Table 4.

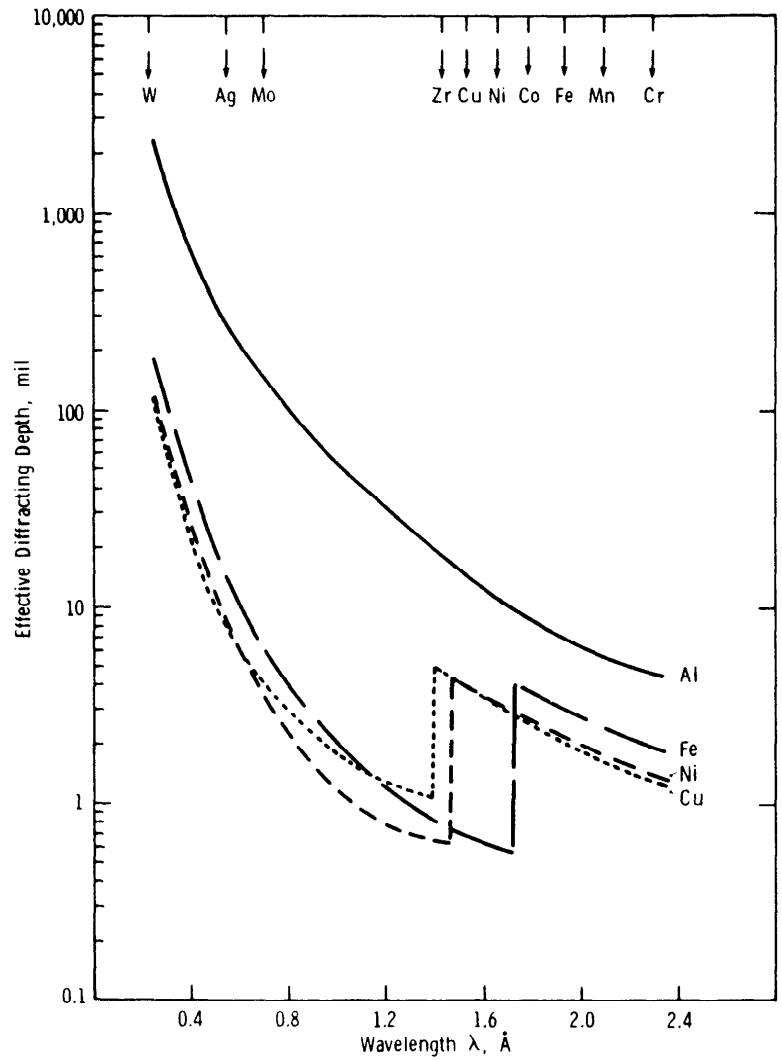

Figure 20. Effective depth of penetration (75% absorption for $\theta = 90^{\circ}$) vs wavelength of X-radiation (part I).

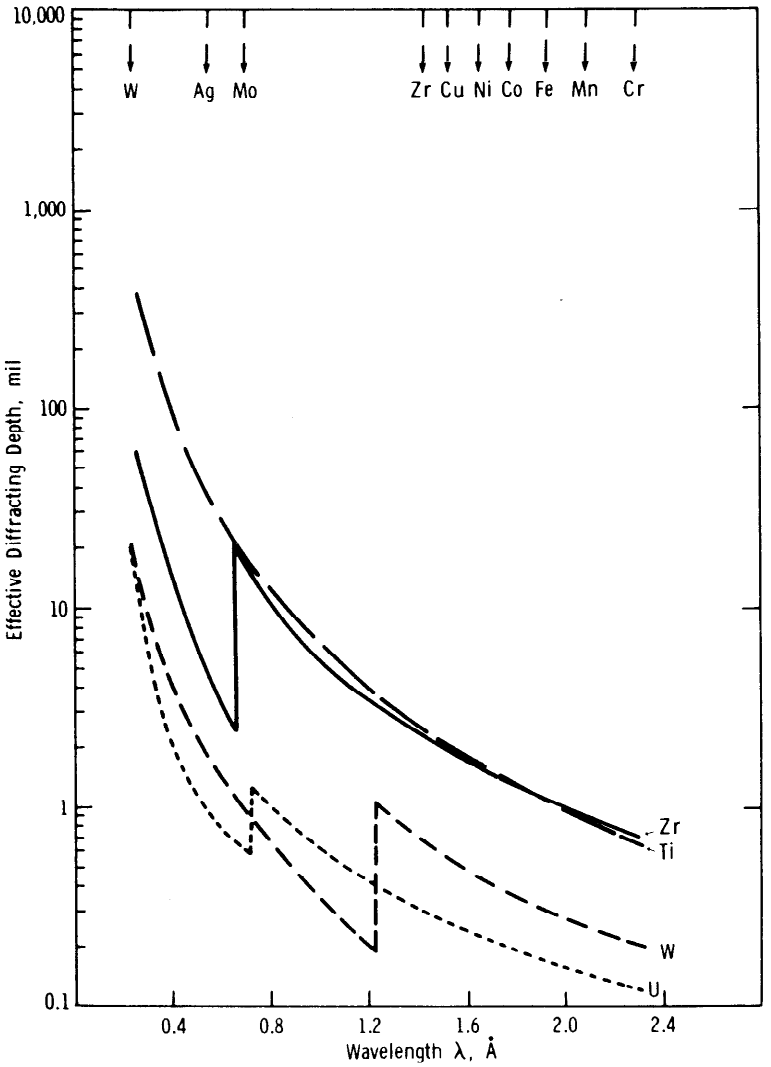

Figure 21. Effective depth of penetration (75% absorption for $\theta = 90^{o}$) vs wavelength of X-radiation (part 2).

APPARATUS

The development of equipment for XRDRSA has taken on many forms. In an X-ray research laboratory it is commonplace to find custom-made equipment, whether in film form or in a diffractometer design. In industry, one usually observes a commercial system that is supplied "off-the-shelf" to perform established and often routine procedures.

The earliest form of X-ray residual stress apparatus is the film camera of Lester and Aborn[7] (see History and Progress). X-ray cameras were used in spite of the fact that diffractometers were developed prior to WW I. This is probably due to the fact that they were cheap and easy to manufacture, afforded the spatial advantage of a position sensitive detector, gave a permanent record of the diffraction conditions, and easily made it possible to obtain precision levels, in keeping with the theoretical development of XRDRSA. In fact, the film camera is yet capable of recording diffraction peaks at higher 2θ positions than with the electronic counter.

Table 3. X-RADIATION (TARGET, K) EMPLOYED IN RESIDUAL STRESS OF MATERIALS (hkl) 2θ

X-RADIATION	Material										
	MG	AL	Ti	Fe_{α}	Fe_{γ}	Ni	Cu	BRASS	ZR	W	U
$CrK\alpha$	(104) 152	(222) 157		(211) 156					(104) 156		(133) 166
$CrK\beta$					(311) 149						
$FeK\alpha$	(105) 166										
$CoK\alpha$		(420) 162	(114) 155	(310) 160			(400) 163	(400) 151 68%Cu			
$NiK\alpha$								(331) 158 (CART)			
$CuK\alpha$		(511) (333) 163	(213) 142		(420) 147	(420) 150 (331) 145	(420) 146			(400) 154 (321) 131	(116) 158 (154) (313) 142

Results of XRDRSA utilizing cameras were obtained and continued throughout the 40's[23] and useful features, such as protractor gauges were introduced[24] and applied to portable systems in later years.[25] Film cameras are still in use and are today being considered for special applications, as in the recording of data where space is a problem, such as XRDRSA in tubes or boreholes.[26]

To trace the evolution of various diffractometer systems may be of interest and provide some rewarding insight regarding the introduction of future systems.

With the introduction of the diffractometer by Christenson and Rowland,[11] the General Electric XRD 3 and subsequent models, such as the XRD 5, were designed to support heavy specimens (up to 90 lb.) in the horizontal mode and were easily adapted to XRDRSA (see Figure 22). In this case, a specimen platform and a variable position detector mount were installed from a design obtained from Syracuse University. (The design dates to 1956 and was kindly furnished to Watertown Arsenal in 1959.) Later,

23. NORTON, J. T., and ROSENTHAL, D. *Stress Measurement by X-ray Diffraction,* Proc. SESA, v. 1, 1943, p. 73.
24. ISENBURGER, H. R. *Stress Analysis by X-ray Diffraction,* Machinery, July 1947, p. 167.
25. BOLSTAD, D. A., and QUIST, W. E. *The Use of a Portable X-ray Unit for Measuring Residual Stresses in Aluminum, Titanium, and Steel Alloys,* Adv. X-ray Anal., v. 8, 1965, p. 26.
26. BORGONOVI, G., EPPERSON, D., HOUGHTON, G., and ORPHAN, V. *Technical Feasibility of a Borehole Probe for In-Situ X-ray Diffraction Analysis,* Adv. X-ray Anal., v. 24, 1981, p. 197.

Table 4. TECHNICAL PROBLEMS

Grain Size:

Diagnosis: Displace specimen laterally (while in diffraction); if intensity changes, grain size problem.

Solutions:

(1) Oscillate film (camera technique)
(2) Oscillate specimen (i.e., ψ direction)
(3) Displace specimen (in plane of specimen)
(4) Make beam larger (i.e., larger beam slit)
(5) Use divergent beam
(6) Use shorter wavelength X-rays.

Texture:

Diagnosis: Intensity of diffraction peak changes with ψ (independently with lateral specimen displacement).

Solutions:

(1) Marion-Cohen correction (phase shift)
(2) Dolle-Cohen {hoo}, {hhh}
(3) Nontexture path (i.e., (310) in steel)
(4) Large divergent beam
(5) Multiple (hkl) peaks (i.e., nondispersive).

Surface Distortion:

Diagnosis: (1) Broad diffraction peak
(2) Suspiciously high compressive stress
(3) Nonlinear $\Delta 2\theta$ vs $\sin^2 \psi$.

Solutions:

(1) Electropolish
(2) Chemical polish
(3) Special mechanical polishing procedure (no cold work)
(4) Use shorter λ.

commercial systems[4] were and are yet commonly employed. Similar horizontal diffractometers, such as those manufactured by Siemens Co., are conducive to such applications, since they possess an independent omega motion, for easily setting the ψ angle (see Figure 23). This system has recently been updated to include a PSD by the Siemens Co.

From the technology of the General Electric XRD series, in the U.S.A., innovations have emerged to increase the speed of operation. The Fastress was designed to independently, but automatically, record two ψ angle, diffraction events simultaneously. Removal of the goniometer from the console provided for semiportable applications, and in some cases, the portability was extended[27] with the use of a fork lift truck.

27. HERFERT, R. E. *Automated Residual Stress Analyzers Using X-ray Diffraction,* Proc. of the Workshop on ND Eval. of Residual Stress, NTIAC-76-2, San Antonio, Tx., 13-14 August 1975, p. 141.

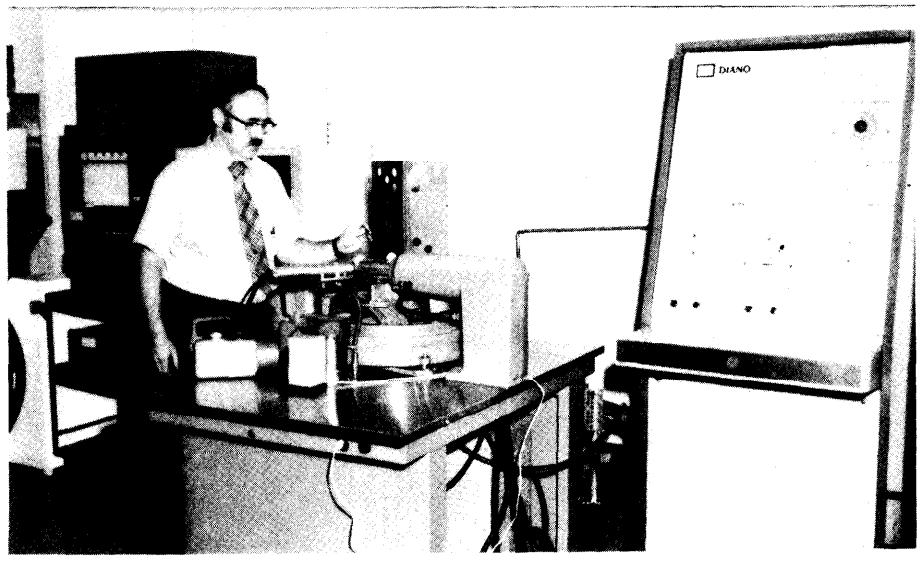

Figure 22. X-ray residual stress measurements with a divergent beam system (G.E./ Diano) and a custom-built specimen and detector supports.

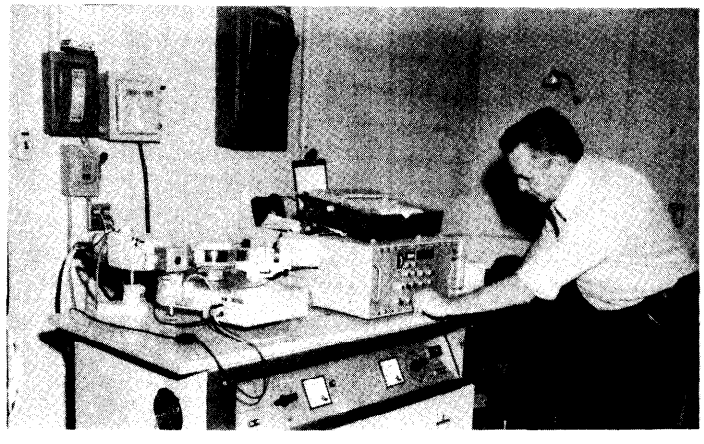

Figure 23. A Siemen's company divergent beam X-ray diffractomer with variable $\omega(\psi)$ motion.

The development of an X-ray stress analyzer in the U.S. Navy followed an interesting course, and the U.S. Navy took the lead in developing an X-ray system. A Siemens diffractometer was automated[28] with customized interfacing, in the early 70's. The U.S. Army patterned a Siemens diffractometer after this system, at the Watervliet Arsenal.[29] The Navy also sponsored the development of a high-speed

28. CANNER, I. *Automated X-ray Diffractometer for Surface Stress Determinations in Structural Components,* 23rd Def. Conf. on NDT, NTIAC, San Francisco, Calif., 4-6 September 1974.
29. CAPSIMALIS, G. P., HAGGERTY, R. F., and LOOMIS, K. *Computer Controlled X-ray Stress Analysis for Inspection of Manufactured Components,* Watervliet Arsenal Rpt. No. WVT-TR-77001, Watervliet, N. Y., January 1977.

portable system, incorporating a proportional wire detector, capable of making measurements in 15-20 sec.[30,31] This system, called "PARS" (Portable X-ray Analyzer for Residual Stresses) was manufactured by the American Analytical Corp., Grafton, Ohio. With modifications and improvements this system will be produced by the Technology for Energy Corp.

Diffraction Geometry

The usual XRDRSA system is dependent on divergent beam focussing. Normally, the electron beam in the X-ray tube is focussed at a line, approximately 1 mm wide by a cm, or so, long. With Bragg-Brentano focussing, the X-ray diffracted is focussed on the focussing circle, for any θ position of the sample and target, (see Figure 24). The receiving slit is adjusted to "scan" across the focal spot position.

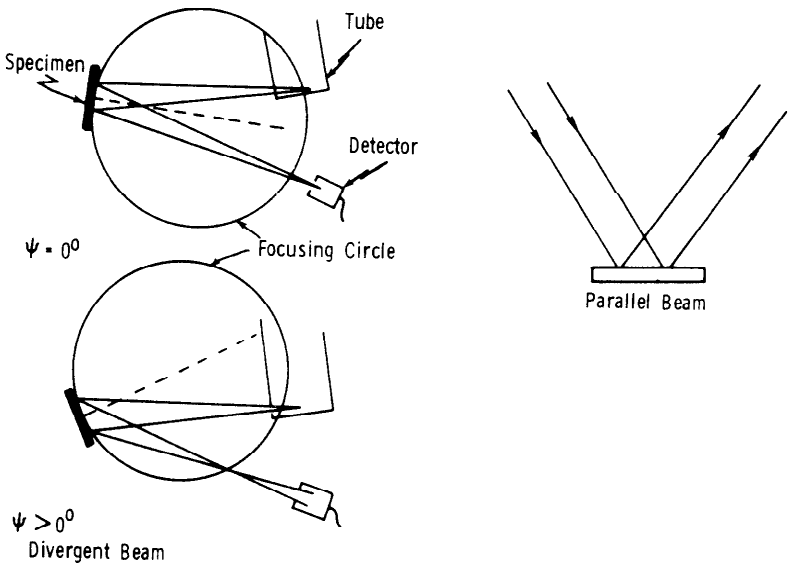

Figure 24. Schematic drawings of the divergent and parallel beam diffraction geometries illustrating the variation of the focal spot (divergent) position and the nonexistence of the focal spot (parallel beam case).

There are definite advantages in this divergent beam geometry, namely:

(1) Flexibility in the adjustment of specimen surface area by means of the beam slit selection,

(2) Large X-ray intensity,

30. JAMES, M. R., and COHEN, J. B. *The Application of a Position Sensitive X-ray Detector to the Measurement of Residual Stresses,* Adv. X-ray Anal., v. 19, 1976, p. 695.
31. JAMES, M. R., and COHEN, J. B. *"PARS" – A Portable X-ray Analyzer for Residual Stresses,* JTEVA, v. 6, 1978, p. 91.

(3) Ability to adjust resolution/intensity by means of a change in the receiving slit width,

(4) Can reduce the "effective grain size" by including a greater distribution of grains with different crystalline orientations, in the diffracting condition. This is also effective for minimizing the texture error when the Marion-Cohen correction is applied.

The alternate geometry is called the parallel beam system. In this case, (see Figure 24), the X-ray beam is collimated to yield an almost parallel incident and diffracted beam. As a result, a high degree of resolution is obtained at the sacrifice of X-ray intensity. This diffraction mode was initiated by the Japanese school in the 60's, and commercial X-ray apparatus is available with this geometry (Rigaku Inc.), and residual stress results can be seen in the literature using such equipment.[27,32] The advantages of parallel beam geometry are:

(1) High resolution or smaller instrumental broadening,

(2) Insensitivity to height displacement of the specimen, or reduction of the positioning error. This allows the investigator to examine specimens with a smaller radius of curvature, or a rougher surface, without sacrificing error,

(3) Fewer slit parameters to consider.

The Rigaku Strainflex, utilizing parallel beam optics (see Figure 25) was evaluated for U.S. Army applications[33] as a laboratory and field instrument (see Figures 26 and 27). This system is automatic, with an oscillation feature ($\pm 3^{o}$, $\pm 5^{o}$, $\pm 7^{o}$) to minimize the effects of grain size.

High-Speed Systems

1. Single-Exposure Method

The assumption that the elastic residual strain is linear with respect to $\sin^2 \psi$, as the basis for the two ψ angle or Glocker Method,[5,9] in principle, is compatable with the single exposure method.[32] As is illustrated in Figure 28, this technique provides two ψ angles from one exposure or diffraction event. This is made possible because a diffraction "ring" or "cone" is produced in powder diffraction, (classically known as a "Debye Ring"). Two opposite sides of the ring are capable of providing two separate ψ values. This means that the data collection time can be cut in half. The disadvantage with this technique is that the choice of the two angles (ψ_1 and ψ_2) is limited. For example, if the Glocker angles of $\psi_1 = 0$ and $\psi_2 = 45^{o}$ were desired, the 2θ angle would have to fortuitously occur at 135^{o}. However, to use the single-exposure method, even if the multiple ψ exposure technique is involved, by selecting the positions of the specimen relative to the X-ray source, a range of ψ's can be selected to provide a statistically meaningful distribution of the elastic strains in almost half the time.

32. CHRENKO, R. M. *X-ray Residual Stress Measurements Using Parallel Beam Optics,* Adv. X-ray Anal., v. 20, 1977, p. 393.
33. GAZZARA, C. P. *A General Purpose Residual Stress Analyzer,* AMMRC TR 83-4, January 1983.

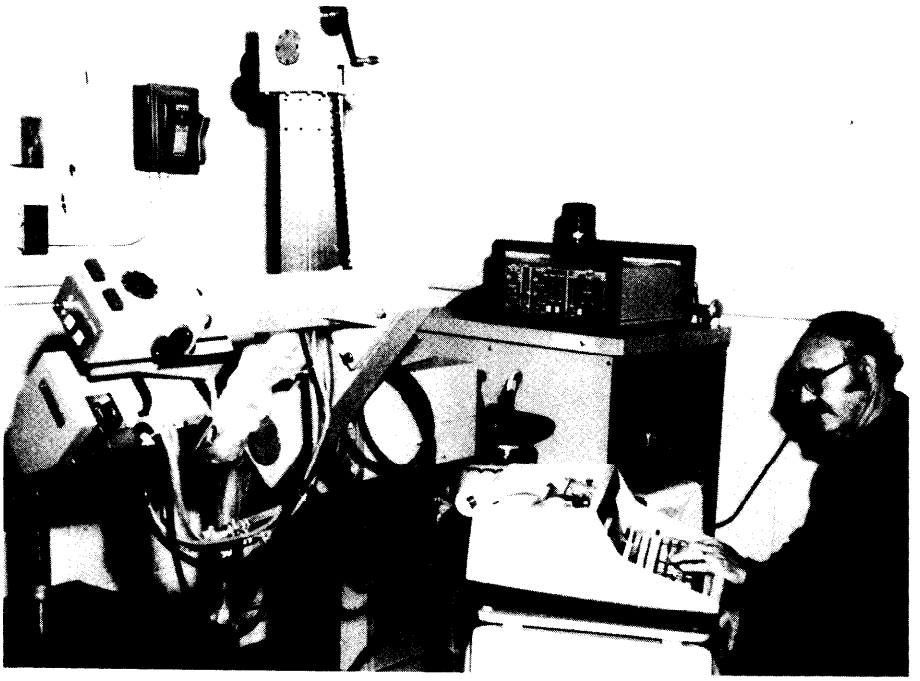

Figure 25. The Rigaku Strainflex residual stress X-ray system with computer controls for laboratory applications.

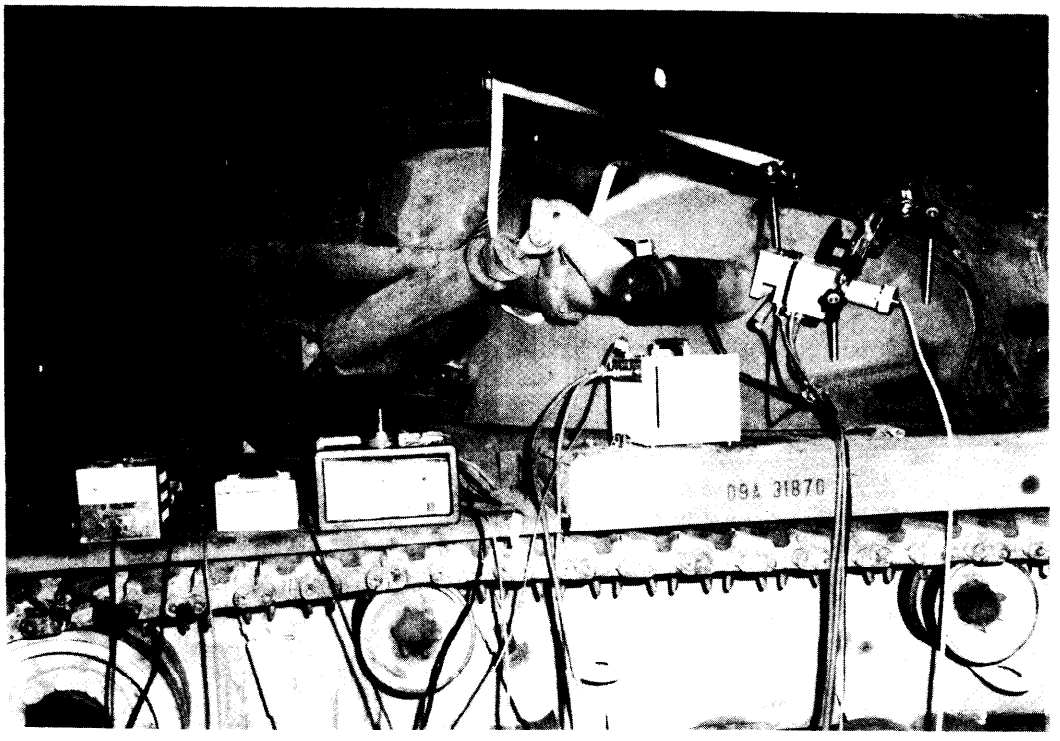

Figure 26. Residual stress field measurements of welds in steel on the M-88 tank retriever with a portable Strainflex X-ray system.

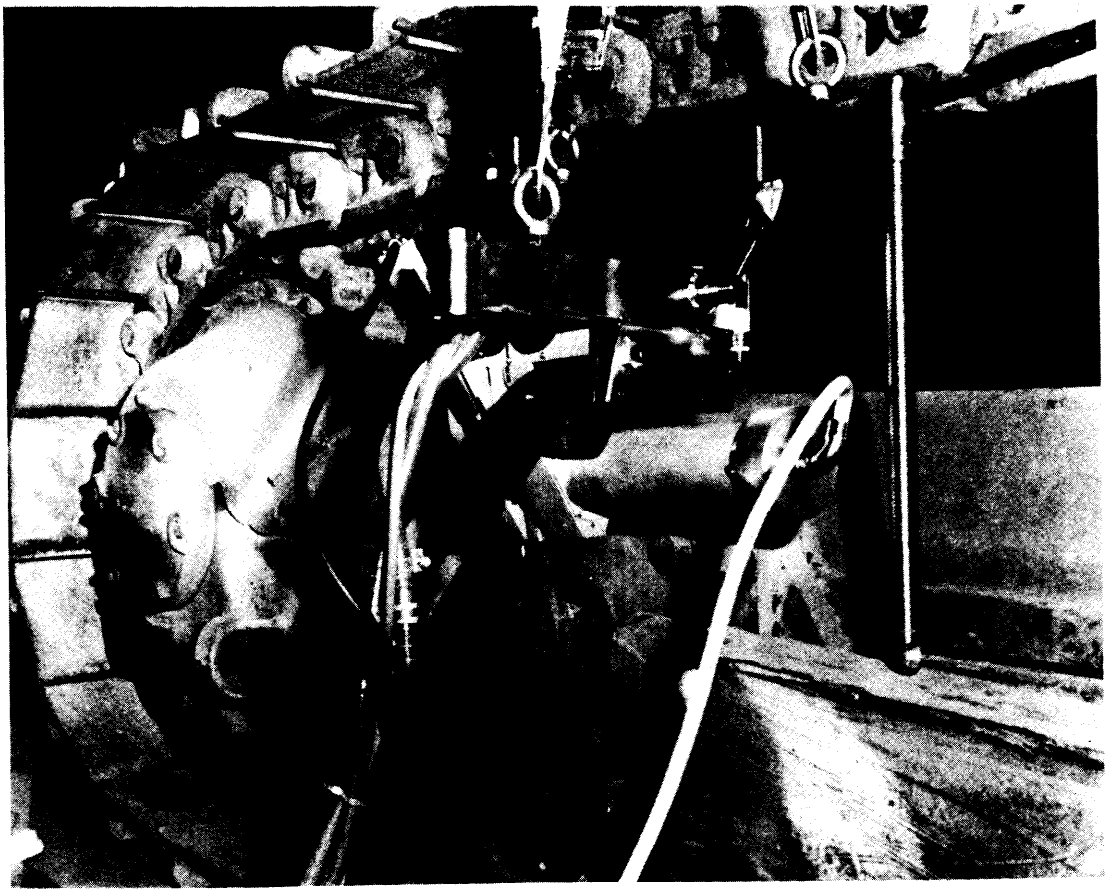

Figure 27. Residual stress field measurements on a steel knuckle of a D-7S bulldozer with a portable Strainflex X-ray system.

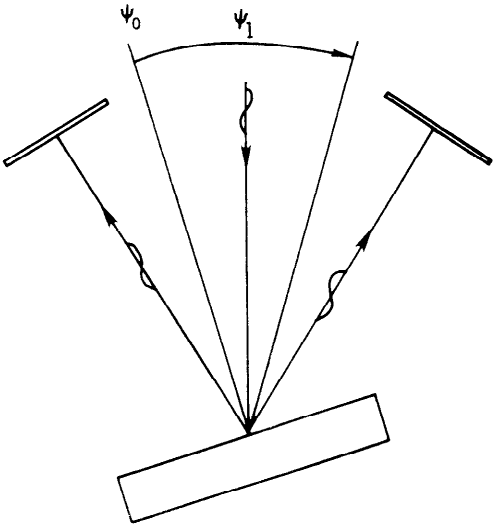

Figure 28. A schematic drawing of the "single exposure" technique for XRDRSA, indicating the arrangement of two simultaneous ψ angles.

The construction of a solid-state PSD[34] to a single-exposure goniometer was performed by the Denver Research Institute (DRI)[35,36] for application to assault bridges at MERADCOM, Fort Belvoir, Va. The scheme of such a system is shown in Figure 29, with the aluminum standard device (see Figure 18) used to evaluate the DRI instrument (see Table 2).[33] Further development of this instrument was transferred to SAI Corp., La Jolla, Calif., with particular application to stress measurements inside stainless steel pipes.[37] This device is being manufactured by Denver X-ray Instruments Inc.[17] However, at this writing, further development is proceeding at Penn State University by Ruud. This series of developmental events, points out that with scientific equipment, in general, many stages in an evolution of improvement, or refinement, occurs (i.e., electron microscope, etc.).

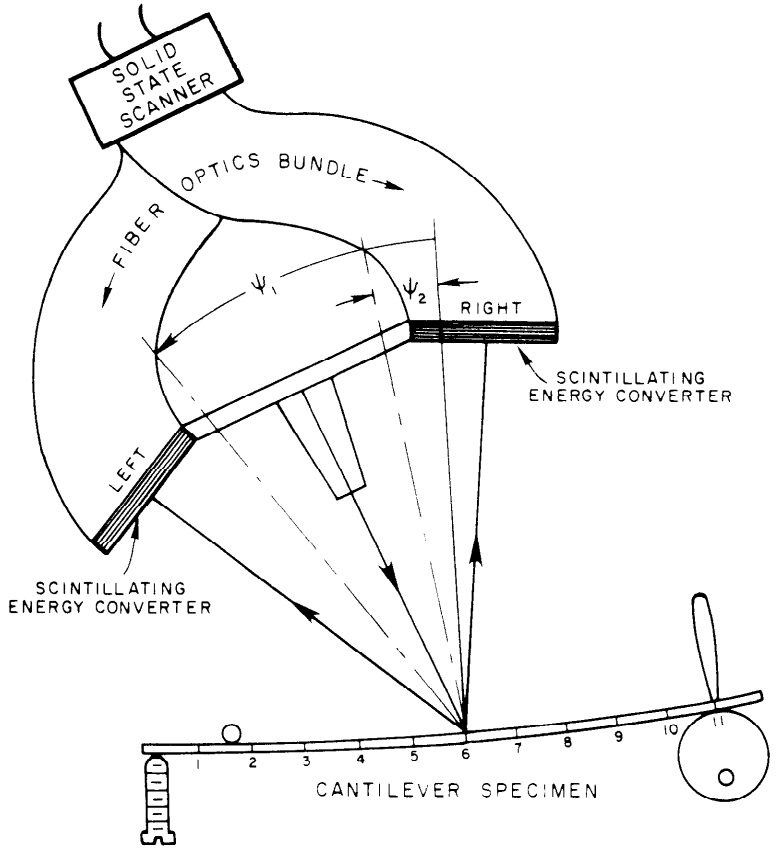

Figure 29. A drawing of the DRI X-ray residual stress single-exposure geometry with an aluminum calibration specimen (see Figure 18).

34. STEFFEN, D. A., and RUUD, C. O. *A Versatile Position Sensitive X-ray Detector,* Adv. X-ray Anal., v. 21, 1978, p. 309.
35. RUUD, C. O., STURM, R. E., and BARRETT, C. S. *A Nondestructive X-ray Instrument to Instantly Measure Residual Stresses,* Type II Interim Tech. Rpt. Phase I, Denver Res. Inst., U.S. Army MERADCOM, Ft. Belvoir, Va.
36. VENDITTI, F. P., STURM, R. E., WARDZALA, E. D., and TEGTMEYER, S. *Prototype Instrument for Instantaneous Measurement of Residual Stresses,* Interim Tech. Rpt. No. 2698, Denver Res. Inst., Denver, Colo., 1979.
37. RUUD, C. O. *Feasibility of Determining Stress in BWR Pipes with the DRI X-ray Stress Analyzer,* EPRI Rpt. NP - 914, October 1978.

2. Multiple-Exposure Method

A similar developmental process took place with the PARS system discussed earlier. The first PARS was designed and constructed at Northwestern U. by James and Cohen,[30,31] subsequently manufactured by the American Analytical Corp., underwent further refinement at Caterpillar Tractor Co., and will be presented to the commercial marketplace as "PARS III" by TEC Corp., Oak Ridge, Tenn. This system permits selection of any angles, ψ_n, to a limiting angle, in a singular progression.

Both high-speed systems incorporate a PSD with effective measurements in 15-20 or more, seconds. A comparison of most of the X-ray systems is given in Table 5. The values listed in Table 5 are approximate, and subject to change, and should only be considered as guidelines.

Future Systems

1. Detection

The advances made in solid-state X-ray detectors (i.e., HgI_2) with increased resolution and efficiency, indicate that reliable room temperature, high-speed detectors are achievable in the near future.

Similar improvements with high-speed solid-state multichannel analyzers will make it possible to perform energy dispersive residual stress analysis, reducing the machining requirements for diffractometers. Conceivably, placing a fixed device against a surface will yield residual stress "readings" in seconds, with corrections for texture, grain size, etc. Much work needs to be done, however, particularly in the energy dispersive curve fitting intensity correction procedures.

2. Intensity

X-ray tube technology will continue to produce new and better X-ray sources. The greatest advances will probably be in producing high-flux tubes with rotating anodes, or pulse sources. A novel method may be to make a target material out of a zero thermal expansion coefficient refractory metal, or ceramic material, permitting high X-ray intensities without the shift in the X-ray focal position and "burnout" (change in depth of the focal spot due to vaporization).

Accelerators or nuclear sources will be limited to laboratory applications but will permit very high energy fluxes for specialized applications.

APPLICATIONS

A summary of the approach to an X-ray diffraction problem was presented at the U.S. Naval Air Rework Facility, San Diego, Calif. on 18-19 November 1981 and is given in Table 6.

Standards

The availability of a reliable standard is important to: (1) ensure that the measured residual stress is related to the mechanical stress, (2) check on changes in the measuring equipment, and (3) calibrate other measuring equipment.

Table 5. COMPARISON OF X-RAY DIFFRACTION RESIDUAL STRESS SYSTEMS

	Rigaku	Fast Stress	DRI	GE/DIANO	Siemens	"PARS" (J.B. Cohen)	Wvlt.	TEC (Hendricks)	Penn St. (Ruud)
Portability	Yes	No	?	No	No	Yes	No	Yes	Semi
Specimen Adaptability	Flexible	Flexible	Flexible	Not Flexible	Flexible	Flexible	Flexible	Flexible	Flexible
Line-up Adaptability	Excellent	Good	Fair	Fair	Fair	Excellent	Fair	Excellent	V. Good
Resolution*	$<0.01^{\circ}$	$<0.01^{\circ}$	0.05°	$<0.01^{\circ}$	$<0.01^{\circ}$	$\sim 0.05^{\circ}$	$<0.01^{\circ}$	>0.02	>0.02
Availability	Yes	Yes	No	?	Yes	?	Custom Made	Special Order	Special Order
2θ Range	$140\text{-}170^{\circ}$	-	$155\text{-}175^{\circ}$	$0\text{-}165^{\circ}$	-	?	$115\text{-}160^{\circ}$	Flexible	Flexible
Reading Time	10 min.	2 min.	20 sec.	20 min. 2 hrs	10 min.	$\sim$20 sec.	15 min. 1 hr.	20 sec.	15 sec.
Setting Angles	Automatic	Automatic	Manual	Manual	Manual	Automatic	Automatic	Automatic	Single Exposure
Specimen Surface	Large 16mm	Small 7mm	v. small 1mm	v. lge. 30mm	-	-	Variable	Variable	Variable
Tube Power	300 watts	1000 watts		1000 watts	1000 watts	150 watts Air Cooled	700 watts	100 watts Air Cooled	<2000 watts H_2O Cooled

* Resolution dependent on distance from target to specimen [TEC and Penn State University have 60μM resolution of detector, same as DRI, PARS-I (180μM)]

Table 6. PROPOSED STEPS FOR APPLICATION OF XRDRSA TO NARF PROBLEMS

Equipment Selection:

(1) Capability (to attack potential problems, i.e., λ, 2θ range, see Table 5)
(2) Adaptability (change with advancing technology, i.e., new computers, monochromators, etc.)
(3) Total systems responsibility (good service)
(4) Off the shelf (includes replacement parts)
(5) Durability, corrosion resistance.

Applications Procedure:

(1) Each problem unique (check grain size, texture, geometry, etc. for each application, see Table 4)
(2) Outline variables (surface condition, hkl, etc.)

Surface conditions:
(a) peak width $\lesssim 1^{\circ}$
(b) $\sigma \approx 30$ ksi compressive-check grinding stress
(c) electropolish- more than 1 mil removal-surface probably cold worked

(3) Establish standards (same composition, grain size, etc.)
(4) Measure residual stress (check linearity of d vs $\sin^2\psi$ if O.K. use Glocker Method)
(5) Determine reproducibility, accuracy, etc.
(6) Fix procedure
(7) When in doubt check standard.

Special Materials:

Aluminum alloys

(a) employ CrKα (222) if possible, i.e. $\psi = 0^{\circ}$, 15°, 30°, 45°
(b) check for grain size effects

Titanium alloys[38,39]

Epoxy composites[39,40]

The characteristics of an acceptable standard are:

(1) Not subject to stress relaxation,

(2) Little chemical reaction of the surface (i.e., oxidation),

(3) Minimum of sharp stress gradients,

(4) Material is the same as the specimen to be examined,

(5) Surface can be placed in proper alignment quickly.

38. BAUCUM, W. *Residual Stress Analysis by X-ray Diffraction,* Union Carbide Rpt. YDA No. 3741, Oak Ridge, Tenn., 1971.
39. BARRETT, C. S. *Diffraction Technique for Stress Measurement in Polymeric Materials,* Adv. X-ray Anal., v. 20, 1977, p. 329.
40. BARRETT, C. S. *X-ray Diffraction Evaluation of Adhesive Bonds and Stress Measurement with Diffracting Paint,* Adv. X-ray Anal., v. 24, 1981, p. 231.

The standards prepared for testing aluminum alloys were illustrated in Figure 18. Here, cantilever specimens, 1 in. wide x 12 in. long, were prepared and deflected a reproducible amount each time measurements were to be taken (to avoid stress relaxation). The results shown in Table 2 indicate the range of stresses available and the effectiveness in testing another X-ray system (DRI).

For the case of steel, a low carbon steel with significant stress levels, was prepared for use as a standard. The sides were machined to within 1^{o} of orthogonality, and the surface finished by a mechanical procedure leaving the surface stress free (see TECHNICAL PROBLEMS, 3. Surface Distortion). The standard was then examined for residual stress levels, checking for texture, grain size and surface effects (see Table 4). In order to check for reproducibility, the measurements were repeated on the Rigaku Strainflex many times and then examined with the divergent beam Diano diffractometer. Measurements on this specimen were repeated at other laboratories, such as: TARADCOM, DRI, G.E. (Schenectady, N.Y.), at Rigaku (Danvers, Mass.), at Bethlehem Steel Co., etc. A schematic drawing of this steel standard, showing the stress readings, can be seen in Figure 30.

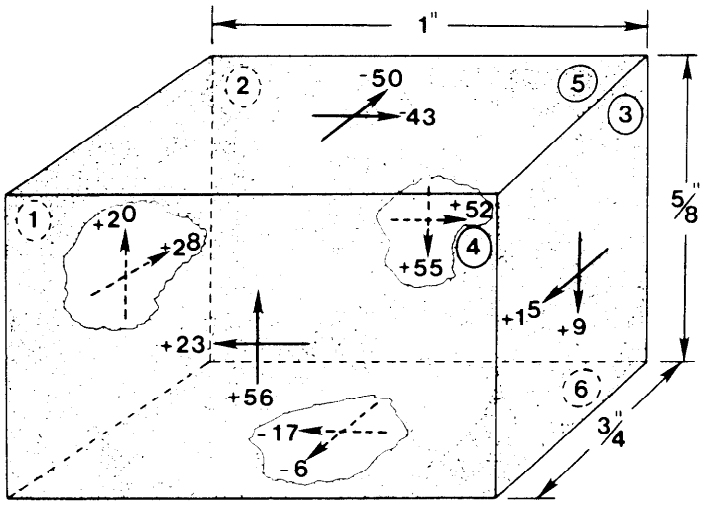

Figure 30. The location and X-ray residual stress values on a steel calibration specimen.

This standard has been applied in the many instances that a steel specimen is to be tested (i.e., M 735 maraging steel sheath, 8-in. shells, MBTA axle [see Figure 19], etc.).

The following example illustrates the importance of a residual stress analysis of a steel specimen. A TOW (tube launched, optically tracked and wire-guided) rocket missile case, was examined* as a step in a failure analysis. The application's

*HICKEY, C. F., HATCH, H., and GAZZARA, C. P. *Residual Stress Analysis Relative to TOW Rocket Motor Case Failures,* AMMRC Letter Report, August 1981.

procedure, in Table 6, was followed with checks for texture effects, grain size problems, etc. Positions along the case were measured with multiple ψ angles, before and after electropolishing. It was concluded that the results, before and after electropolishing, were the same, that no effects due to texture nor large grain size were evident, that the strain was linear in $\sin^2 \psi$, and that the measured residual stress values were reproducible.

An interesting time-saving procedure was taken (in addition to being able to use the Glocker Method), namely: the faster Barkhausen test method, which although not quantitatively reliable, could serve to ensure a constant level of stress around the TOW cases. Therefore, the measurement of residual stresses around the cases was quickly found to be unnecessary. The results of a TOW XRDRSA is shown in Figure 31. Notice the high tensile stresses found near the posterior trouble area.

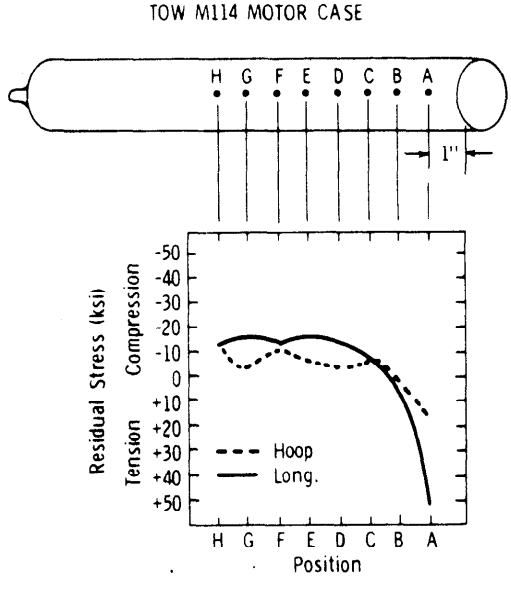

Figure 31. Residual stress measurement using a Strainflex automatic ($\psi_o' = 0, 15, 30, 45^o$) of a TOW M-114 maraging steel motor case (as-received).

A point worth emphasizing is that once the procedure for measuring residual stresses has been established, in a specimen such as a TOW case, that in making measurements in the future, use could be made of this shorter, reliable X-ray method, providing that processing of the item has not been drastically changed.[41]

41. PUTUKIAN, J. *Annotated Bibliography for Nondestructive Measurement of Wheel/Axle Residual Stress (1969-1981),* Rpt. No. RR 128 - PM - 81, v. 26, DOT, Cambridge, Mass., June 1981.

REFERENCES

1. CULLITY, B. D. *Elements of X-ray Diffraction,* Addison Wesley, Reading, Mass., 1967.
2. FRIEDRICH, W., KNIPPING, P., and VON LAUE, M. *Interferenz-Erscheingen bei Rontgenstrahlen,* Ber. bayer. Akad. Wiss., 1912, p. 303.
3. BRAGG, W. L. *The Diffraction of Short Electromagnetic Waves by a Crystal,* Proc. Camb. Phil. Soc., v. 17, 1912, p. 43.
4. *Residual Stress Measurement by X-ray Diffraction,* SAEJ784a, Soc. of Aut. Engrs. Inc., Warrendale, Pa., 1971.
5. HULL, A. W. *The Crystal Structure of Iron,* Phys. Rev., v. 9, 1917, p. 84.
6. DEBYE, P., and SHERRER, P. *Interferenz an regellos orientierten Tielchen im Rontgenlicht I.,* Phys. Zeits., v. 17, 1916, p. 277.
7. LESTER, H. H., and ABORN, R. H. *Behavior Under Stress of the Iron Crystals,* Army Ordnance, v. 6, 1925, 1926, pp. 120, 200, 283, 364.
8. HASKEL, R. K. *X-ray Diffraction as Applied to the Determination of Stress Conditions in Gun Steel,* Watertown Arsenal Rpt. No. 160/2, Watertown, Mass., 1934.
9. GLOCKER, R., and OSSWALD, E. *Unique Determination of the Principal Stresses with X-rays,* Z. Tech. Physik, v. 161, 1935, p. 237.
10. MOLLER, H., and BARBERS, J. *X-ray Investigation of the Stress Distribution and Overstraining in Ingot Steel,* Mitt. Kaiser-Wilhelm-Inst., EisenForsch, Dusseldorf, v. 16, 1934, p. 21.
11. CHRISTENSON, A., and ROWLAND, E. *X-ray Measurement of Residual Stress in Hardened High Carbon Steel,* Trans. Am. Soc. Metals, v. 45, 1953, p. 638.
12. WEIDEMANN, W. *PhD. Thesis,* Technische Hochschule, Aschen, Germany, 1966, synopsis in Reference 13. Also published with BOLLENROTH, V. F., and HAUK, V. *Zur Dentung der Gittereigenverformungen in Plastich Verformtem-Eisen,* Arch. fur Eisen, v. 10, 1967, p. 793.
13. MARION, R. H., and COHEN, J. B. *Anomalies in Measurement of Residual Stress by X-ray Diffraction,* Adv. X-ray Anal., v. 18, 1975, p. 466.
14. DÖLLE, H. *The Influence of Multiaxial Stress States, Stress Gradients, and Elastic Anisotropy on the Evaluation of Residual Stresses by X-rays,* J. Appl. Cryst., v. 12, 1979, p. 489.
15. DÖLLE, H., and COHEN, J. B. *Evaluation of Residual Stresses in Textured Cubic Metals,* Met. Trans. A., v. 11A, 1980, p. 831.
16. BECHTOLDT, C. J., PLACIOUS, R. C., BOETTINGER, W. J., and KURIYAMA, M. *X-ray Residual Stress Mapping in Industrial Materials by Energy Dispersive Diffractometry,* Adv. X-ray Anal., v. 25, 1982.
17. RUUD, C. O. *Review and Evaluation of Nondestructive Methods for Residual Stress Measurement,* Elec. Pwr. Res. Inst. Rpt. NP-1971, Proj. 1395-5, September, 1981.
18. GAZZARA, C. P. *The Measurement of X-ray Residual Stress in Textured Cubic Materials,* Proc. Fall Mtg. SESA, Keystone, Colo., 11-14 October 1981, p. 32.
19. HORNUNG, N. L. *X-ray Stress Analysis Development of Aluminum Standards,* Spec. AMMRC Tech. Rpt. (in print).
20. LETNER, H. R. *Influence of Grinding Fluids Upon Residual Stresses in Hardened Steel,* ASME Trans., v. 79, 1957, p. 149.
21. FOPIANO, P. J., and ZANI, A. J. *Metallographic Preparation of Two-Phase Titanium Alloys for Replica Electron Microscopy,* Metallography, v. 3, 1970, p. 209.
22. MIDDLETON, R. M., and HICKEY, C. F. *Transformation Characteristics of Transage Ti 129,* Titanium and Titanium Alloys-Scientific and Technological Aspects, J. C. WILLIAMS and A. F. BELOV, eds., Plenum Press, N.Y., 1981.
23. NORTON, J. T., and ROSENTHAL, D. *Stress Measurement by X-ray Diffraction,* Proc. SESA, v. 1, 1943, p. 73.
24. ISENBURGER, H. R. *Stress Analysis by X-ray Diffraction,* Machinery, July 1947, p. 167.
25. BOLSTAD, D. A., and QUIST, W. E. *The Use of a Portable X-ray Unit for Measuring Residual Stresses in Aluminum, Titanium, and Steel Alloys,* Adv. X-ray Anal., v. 8, 1965, p. 26.
26. BORGONOVI, G., EPPERSON, D., HOUGHTON, G., and ORPHAN, V. *Technical Feasibility of a Borehole Probe for In-Situ X-ray Diffraction Analysis,* Adv. X-ray Anal., v. 24, 1981, p. 197.
27. HERFERT, R. E. *Automated Residual Stress Analyzers Using X-ray Diffraction,* Proc. of the Workshop on ND Eval. of Residual Stress, NTIAC-76-2, San Antonio, Tx., 13-14 August 1975, p. 141.
28. CANNER, I. *Automated X-ray Diffractometer for Surface Stress Determinations in Structural Components,* 23rd Def. Conf. on NDT, NTIAC, San Francisco, Calif., 4-6 September 1974.
29. CAPSIMALIS, G. P., HAGGERTY, R. F., and LOOMIS, K. *Computer Controlled X-ray Stress Analysis for Inspection of Manufactured Components,* Watervliet Arsenal Rpt. No. WVT-TR-77001, Watervliet, N. Y., January 1977.
30. JAMES, M. R., and COHEN, J. B. *The Application of a Position Sensitive X-ray Detector to the Measurement of Residual Stresses,* Adv. X-ray Anal., v. 19, 1976, p. 695.
31. JAMES, M. R., and COHEN, J. B. *"PARS" – A Portable X-ray Analyzer for Residual Stresses,* JTEVA, v. 6, 1978, p. 91.
32. CHRENKO, R. M. *X-ray Residual Stress Measurements Using Parallel Beam Optics,* Adv. X-ray Anal., v. 20, 1977, p. 393.
33. GAZZARA, C. P. *A General Purpose Residual Stress Analyzer,* AMMRC TR 83-4, January 1983.
34. STEFFEN, D. A., and RUUD, C. O. *A Versatile Position Sensitive X-ray Detector,* Adv. X-ray Anal., v. 21, 1978, p. 309.
35. RUUD, C. O., STURM, R. E., and BARRETT, C. S. *A Nondestructive X-ray Instrument to Instantly Measure Residual Stresses,* Type II Interim Tech. Rpt. Phase I, Denver Res. Inst., U.S. Army MERADCOM, Ft. Belvoir, Va.
36. VENDITTI, F. P., STURM, R. E., WARDZALA, E. D., and TEGTMEYER, S. *Prototype Instrument for Instantaneous Measurement of Residual Stresses,* Interim Tech. Rpt. No. 2698, Denver Res. Inst., Denver, Colo., 1979.
37. RUUD, C. O. *Feasibility of Determining Stress in BWR Pipes with the DRI X-ray Stress Analyzer,* EPRI Rpt. NP - 914, October 1978.
38. BAUCUM, W. *Residual Stress Analysis by X-ray Diffraction,* Union Carbide Rpt. YDA No. 3741, Oak Ridge, Tenn., 1971.
39. BARRETT, C. S. *Diffraction Technique for Stress Measurement in Polymeric Materials,* Adv. X-ray Anal., v. 20, 1977, p. 329.
40. BARRETT, C. S. *X-ray Diffraction Evaluation of Adhesive Bonds and Stress Measurement with Diffracting Paint,* Adv. X-ray Anal., v. 24, 1981, p. 231.
41. PUTUKIAN, J. *Annotated Bibliography for Nondestructive Measurement of Wheel/Axle Residual Stress (1969-1981),* Rpt. No. RR 128 - PM - 81, v. 26, DOT, Cambridge, Mass., June 1981.